# Chem Soc Rev



# **REVIEW ARTICLE**

**View Article Online** 



Cite this: Chem. Soc. Rev., 2022, **51**, 1702

Received 15th December 2021 DOI: 10.1039/d1cs01074c

rsc.li/chem-soc-rev

# Nanodiscs: a versatile nanocarrier platform for cancer diagnosis and treatment

Jitender Bariwal, 🗓 Hairong Ma, Guillermo A. Altenberg and Hongjun Liang 🗓 \*

Cancer therapy is a significant challenge due to insufficient drug delivery to the cancer cells and nonselective killing of healthy cells by most chemotherapy agents. Nano-formulations have shown great promise for targeted drug delivery with improved efficiency. The shape and size of nanocarriers significantly affect their transport inside the body and internalization into the cancer cells. Non-spherical nanoparticles have shown prolonged blood circulation half-lives and higher cellular internalization frequency than spherical ones. Nanodiscs are desirable nano-formulations that demonstrate enhanced anisotropic character and versatile functionalization potential. Here, we review the recent development of theranostic nanodiscs for cancer mitigation ranging from traditional lipid nanodiscs encased by membrane scaffold proteins to newer nanodiscs where either the membrane scaffold proteins or the lipid bilayers themselves are replaced with their synthetic analogues. We first discuss early cancer detection enabled by nanodiscs. We then explain different strategies that have been explored to carry a wide range of payloads for chemotherapy, cancer gene therapy, and cancer vaccines. Finally, we discuss recent progress on organic-inorganic hybrid nanodiscs and polymer nanodiscs that have the potential to overcome the inherent instability problem of lipid nanodiscs.

## 1. Introduction

Circulating chemotherapeutics are significantly affected by their physicochemical properties (solubility, stability, pH,

Department of Cell Physiology and Molecular Biophysics, and Center for Membrane Protein Research, School of Medicine, Texas Tech University Health Sciences Center, Lubbock, TX, USA. E-mail: H.Liang@ttuhsc.edu

etc.), pharmaceutical properties (release profile, target specificity, etc.), and biological barriers (dense desmoplasia, high interstitial pressure, blood-brain barrier, etc.). The tumor microenvironment (TME) presents an unprecedented complex barrier for chemotherapeutics to reach deep-seated cancer cells in solid tumors. The complex TME consists of the cancer cells as well as the endothelial, mesenchymal, and immune cells that are recruited to the tumor bed to help develop tumor



Jitender Bariwal

Jitender Bariwal received his PhD degree in Pharmaceutical Sciences from Saurashtra University, Rajkot, India in 2009 under the supervision of Prof. Kishor S. Jain and Prof. Anamik K. Shah. He worked as a Post Doctorate researcher with Prof. Erik Van der Eycken (2009 to 2010) at KU Leuven, with Prof. Ram I. Mahato (2017-2020) at UNMC, Omaha and currently with Prof. Hongjun Liang at TTUHSC, Lubbock from 2020. His current research interest

includes synthesis of new polymers using different polymerization techniques for drug delivery applications for cancer mitigation and development of new antibacterial polymer brushes.



Hairong Ma

Hairong Ma received her PhD in Biophysics from University of Illinois Urbana-Champaign in 2005 under the supervision of Prof. Martin Gruebele. She worked as a Postdoc with Prof. Ahmed Zewail at California Institute of Technology (2005-2008), and with Profs Ralph Jimenez and Amy E. Palmer at JILA, University of Colorado-Boulder (2008-2012). She subsequently joined the Department of Physics at Drexel University as a tenure-

track Assistant Professor, and resigned from Drexel in 2015 to join Texas Tech University Health Sciences Center. Her current research interest is on antimicrobials and drug delivery.

**Review Article** 

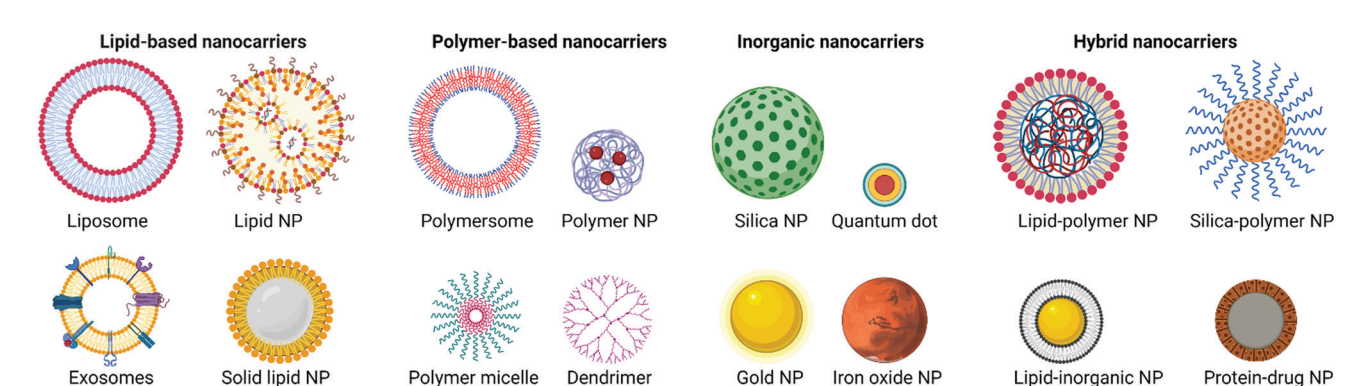


Fig. 1 Different classes of nanocarriers. Each class features multiple subclasses, with some of the most common subclasses highlighted here.

stroma. Together with the extracellular matrix, they form a strong barrier for chemotherapeutics, resulting in suboptimal therapeutic effects and toxicities such as cardiotoxicity, nephrotoxicity, myelosuppression, and other side effects.2 The suboptimal chemotherapeutic concentration likely helps the development of drug resistance.3 Incessant advancement in the molecular biology of TME and new anticancer agents including chemotherapy molecules, antibodies, siRNAs, miRNAs, plasmid DNA, peptides, and engineered immune cells continue to offer new and effective treatment options. However, their effectiveness is often not translated into clinical therapeutic breakthroughs due to the lack of efficient delivery systems.

Nanomedicines have great potential for cancer mitigation. They alter the pharmacokinetics of anticancer drugs, improve stability, provide specific targeting, exhibit a high surface-tovolume ratio, control drug release, and re-model immunosuppressive TME.4 Compared to conventional formulations, nano-formulations (i.e., nanoparticle-based drug delivery carriers) rely on functional nanomaterials to realize on-demand drug release in a precise manner in response to internal stimuli (such as redox or oxidative environments, pH stimuli, tumor-specific enzymes) or external triggers (such as UV or infra-red light, temperature and ultrasound, electric and magnetic fields). 1,5,6 Nanocarriers have been shown to significantly improve the delivery of hydrophobic chemotherapy agents by enhancing their bioavailability and protecting them from various enzymes and other destabilizing factors.7 They have also been widely used for the delivery of hydrophilic molecules like small organic molecule as well as large biomolecules like siRNA, mRNA and miRNA.8-11

The nanocarriers for anticancer drug delivery are broadly classified in four main categories, i.e., lipid-based, polymerbased, inorganic, and hybrid nanocarriers. Each class of nanocarriers consists of multiple subclasses, among them some of the most common subclasses are presented in Fig. 1. Each class has its own advantages and disadvantages regarding cargo carrying efficiency, stability, and patient response. For more detailed discussions about these nanocarriers, we direct the readers to some excellent reviews in the literatures. 12,13

The development of nanocarriers may be subdivided into two major generations. The first-generation mainly aims to improve the water solubility of hydrophobic drugs and reduce their toxicities/adverse events, e.g., encapsulation of drugs in lipids or



Guillermo A. Altenberg

Guillermo Altenberg received his MD (1983) and PhD (1987) degrees from the University of Buenos Aires and was a postdoctoral fellow working with Professor Luis Reuss at the University of Texas Medical Branch at Galveston from 1988 to 1992. There, he started his academic career in the Department of Neuroscience and Cell Biology, where he stayed until 2007, when he moved to Texas Tech University Health Sciences

Center, where he was Director of the Center for Membrane Protein Research and served as Chair of the Department of Cell Physiology and Molecular Biophysics between 2014 and 2021.



**Hongjun Liang** 

Hongjun Liang received his PhD Materials Science Engineering from University of Illinois Urbana-Champaign in 2005 under the supervision of Prof. Gerard C.L. Wong. He worked as a Postdoc with Prof. Galen D. Stucky at University of California, Santa Barbara (2005-2008), and subsequently joined the Department of Metallurgical and Materials Engineering at Colorado School of Mines as a tenure-track Assistant Professor.

In 2015 he moved to the School of Medicine at Texas Tech University Health Sciences Center as an Associate Professor. His research interest is on theranostic nanodiscs, proteopolymer membranes, and membrane-active antimicrobials.

albumin protein nanostructures, including simple liposomes (LIP) and other lipid vesicles shielded with polyethylene glycol (PEG) to prevent immune response and/or prolong circulation time. Those nanocarriers generally have controlled nanoparticle (NP) sizes that solely depend on the passive enhanced permeability and retention (EPR) effect for cellular distribution, such as the formulations of doxorubicin (DOX) (Doxil, Epegylated LIP) and paclitaxel (PTX) (Abraxane, albumin-bound NP) approved by the Food and Drug Administration (FDA) for clinical use. The second-generation nanocarriers not only provide the benefits of first-generation formulations but also actively search for tumors in vivo. Importantly, they allow tumor imaging, in vivo real-time tracking, and monitoring of the therapeutic efficiency of drugs. 14,15

Additionally, they use tissue-specific ligand coatings to target tumors with on-demand payload release (such as ThermoDox $^{\textcircled{\tiny{\$}}}$ ) to provide increased drug accumulation at the tumor sites.

The last two decades have witnessed extensive developments in both generations of nanocarriers that either physically encapsulate or chemically conjugate anti-cancer drugs, such as LIPs, polymeric nanocarriers, polymer-drug conjugates, lipid-drug conjugates, lipid-polymer conjugates, and inorganic nanocarriers including noble metals, silicon, silica, or iron oxide. Many of these nanocarriers are currently under clinical trials, with some being approved by the FDA for clinical use. A partial list of clinically approved nanocarriers for cancer chemotherapy or diagnosis is provided in Table 1.

Table 1 A partial list of clinically approved nanomedicines for cancer chemotherapy or diagnosis

					Clinical trial	Year of	
No.	Name	Composition	Drug tested	Target cancer	phase	approval	Ref.
Natu	ral/synthetic polymer-based n						
1	Eligard <sup>®</sup>	(PLGH (poly(dl-	Leuprolide acetate	Prostate cancer	_	2002	19
_	(Tolmar)	lactide-co-glycolide)))					
2	Oncaspar	Polymer protein conjugate	L-asparaginase	Leukemia	_	2006	21
3	Genexol-PM	PEG-poly(D,L-lactide) based micelle	Paclitaxel	Breast cancer	_	2007	15
4	Apealea	Micellar	Paclitaxel	Ovarian cancer, peritoneal cancer, and fallopian tube cancer	_	2018	22
Drug	-lipid conjugates						
1	DHP107	Lipid nanoparticle	Paclitaxel	Gastric cancer	_	2016	15
2	PICN	Nanosuspension	Paclitaxel	Breast cancer	_	2014	15
	some formulations combined						
1	DaunoXome <sup>®</sup> (Galen)	Liposomal	Daunorubicin	Karposi's Sarcoma	_	1996	19
2	DepoCyt <sup>©</sup> (Sigma-Tau)	Liposomal	Cytarabine	Lymphomatous meningitis	_	1999	19
3	Marqibo <sup>®</sup> (Onco TCS)	Liposomal	Vincristine	Acute lymphoblastic leukemia	_	2012	19
4	Onivyde <sup>®</sup> (Merrimack)	Pegylated liposomal	Irinotecan	Pancreatic cancer	_	2015	19
5	Doxil <sup>®</sup> /Caelyx <sup>™</sup>	Pegylated liposomal	Doxorubicin	Kaposi's sarcoma	_	1995	19
	(Janssen)	87		Ovarian cancer	_	2005	
	,			Multiple myeloma	_	2008	
6	ThermoDox	Heat-sensitive liposome	Doxorubicin	Hepatocellular carcinoma	Phase III	_	21
7	Myocet	Liposomal	Doxorubicin	Breast cancer	_	2000	15
8	Lipusu	Liposomal	Paclitaxel	Breast and non-small- cell lung cancer	_	2007	15
9	Mepact	Liposomal	Mifamurtide	Osteogenic sarcoma	_	2009	15
10	Vyxeos	Liposomal	Daunorubicin and cytarabine	Leukemia	_	2017	15
11	Mifamurtide (Mepact)	Liposome	Muramyl tripeptide phosphatidyl- ethanolamine	Nonmetastatic, resectable osteosarcoma	_	2009	21
	ein nanoparticles combined w						
1	Abraxane <sup>®</sup> /ABI-007	Albumin-bound	Paclitaxel	Breast cancer	_	2005	19
	(Celgene)	nanoparticles		NSCLC	_	2012	
_	0 1 B (-1 1 - )			Pancreatic cancer	_	2013	
2	Ontak <sup>®</sup> (Eisai Inc)	Engineered protein	IL-2 and diphtheria toxin	Cutaneous T-cell lymphoma	_	2008	19
3	Nab-rapamycin (ABI-009)	Albumin NP	Rapamycin	Advanced malignant PEComa and advanced cancer with mTOR mutations	Phase II	_	21
	ganic and metallic nanopartic Nanotherm $^{ ext{ iny B}}$ (MagForce)	ies Iron oxide		Glioblastoma		2010	15 1
1 2	GastroMARK™; Lumirem®	SPION coated	_	Imaging agent	_	2018 2001	15,19
<i>L</i>	(AMAG pharmaceuticals)	with silicone	_	imaging agent	_	2001	19

**Review Article** Chem Soc Rev

The majority of nanocarriers under development for anticancer drug delivery are spherical in shape. In recent years, non-spherical nanocarriers such as nanodiscs (NDs) have attracted much attention. The idea of ND constitution is inspired from the biologically-derived solutions for the transportation of lipids - which are poorly water-soluble - in blood streams. Among various lipid nanocarriers in human blood, High-Density Lipoproteins (HDLs) plays a crucial role in transportation and metabolism of lipids, particularly cholesterol and triglycerides.<sup>23</sup> HDLs were first isolated in 1929 from equine serum and 1950s from human serum, subsequently, in 1966 it was established that HDLs deficiency might lead to ischaemic heart diseases (IHDs) and later on in mid-1970s, it was confirmed that low plasma HDL levels accelerate the development of atherosclerosis and IHDs due to reduced clearance of cholesterol from the blood vessels.24 HDLs are known to transport signaling lipids, proteins, and microRNAs throughout the body and play multiple functions in complex intercellular communications.<sup>25</sup> These features, particularly the fact that nascent HDLs are essentially NDs encased by amphipathic apolipoproteins, have attracted much attention to develop HDLs and NDs as nanocarriers for various therapeutic agents.

In a broad view, NDs represent a patch of any nanoscale membrane encased by amphipathic molecules such as proteins, synthetic polymers, or short-chain lipids. Depending on the composition of the NDs, they may be classified into four categories (Fig. 2):

- (1) Lipid nanodiscs (LNDs). LNDs consist of a disc-shaped lipid bilayer (typical diameter ~10-20 nm) surrounded and stabilized by amphiphilic biomacromolecules such as Apolipoprotein A1 (apoA-1) or membrane scaffold proteins (MSPs; Fig. 2A), <sup>28,29</sup> saposin, <sup>30</sup> peptides, <sup>31</sup> or nucleic acids; <sup>32</sup>
- (2) Styrene-maleic acid (SMA) lipid nanoparticles (SMALPs), which differ from LNDs in that the amphiphilic membrane scaffold biomacromolecules in LNDs are replaced with synthetic SMA or SMA-like copolymers (Fig. 2B);<sup>33-37</sup>
- (3) Polymer nanodiscs (PNDs). PNDs differs from LNDs in that the lipid bilayer of LNDs is replaced by a synthetic membrane patch consisting of amphiphilic block copolymers,

whereas the same choices of membrane scaffold polymers or biomacromolecules such as MSPs are used (Fig. 2C);<sup>36</sup>

(4) Hybrid nanodiscs (HNDs) or hybrid bicelles. These discshaped nanostructures are not stabilized by amphiphilic macromolecules. Instead, they are made of long-chain cerasome-forming lipids (CFL) and short-chain phospholipids. 27 (Fig. 2D).

Although there are extensive reviews available on nanomedicines for cancer therapy that described the concepts, challenges, and opportunities, 1,2,7,38,39 optimization strategies, 40 nano-formulation for cancer immunotherapy, 4,41,42 and nucleic acid delivery,43 along with specific reviews on LIPs44,45 or micelle-based nano-formulations, 46,47 and reviews that focused extensively on the biological background, isolation, and characterization of LNDs as delivery vehicles for small molecules and siRNA, 23,48-57 very few reviews discussed the development of NDs for cancer diagnosis and treatment. This review intends to provide an overview of recent advances that explore NDs for cancer therapy and present an outlook on future development.

## 2. NDs vs. traditional nanocarriers

The shape and size of NPs has a significant effect on their blood circulation time and cellular internalization. 58-63 Before transvascular transport, a pivotal step is margination (radial drift) of NPs towards the blood vessel walls. The meaningful margination is an essential requirement for the transportation of NPs across the blood vessel. In contrast to spherical NPs, oblate shaped NPs experience torques in the blood flow, resulting in tumbling, rotation, and increased margination towards the blood vessel walls<sup>64-67</sup> (Fig. 3A).

After margination, the transvascular transport is governed by many factors like fluid flow rate, filtration along a capillary and hydrostatic pressure gradient, particularly pressure difference between the vascular pressure and interstitial flow pressure.68 Once these factors are overcome by the NPs, they are transported in the cancer cells through macropinocytosis, clathrin-mediated endocytosis, caveolae-mediated endocytosis, and clathrin-caveolae or dynamin-independent endocytosis

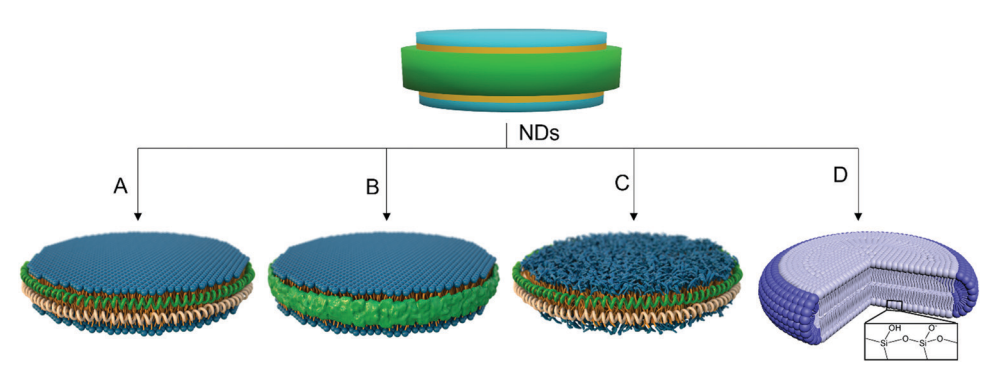


Fig. 2 Various ND platforms for cancer imaging and mitigation. Examples include (A) LNDs encased by MSPs, 26 (B) SMALPs stabilized by amphiphilic SMA-like random copolymers, 26 (C) PNDs encased by MSPs, which differs from LNDs in that the lipid bilayer patch in LNDs is replaced with an amphiphilic block copolymer membrane, <sup>26</sup> and (D) HNDs made from CFL and short-chain phospholipids. <sup>27</sup> Schematic representations of LNDs, SMALPs, PNDs, and HNDs are reproduced with permissions from ref. 26 Copyright 2020, Frontiers Media S. A. and ref. 27 Copyright 2017, John Wiley and Sons.

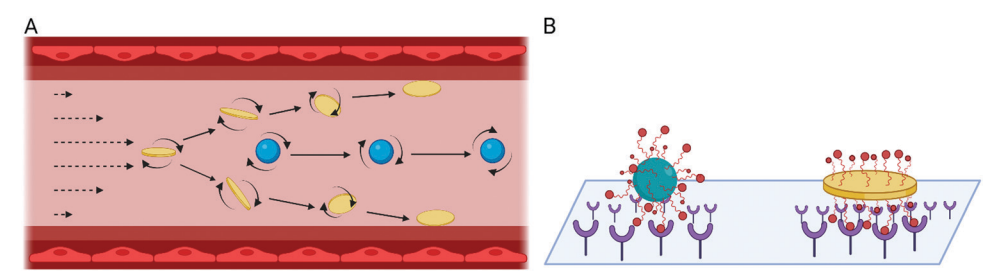


Fig. 3 Effects of particles shape on their margination in the blood flow and binding strength to the endothelium (illustrations adapted from ref. <sup>67</sup>). (A) Margination. NDs are subjected to torque forces within blood flow, experience drift and tend to tumble out of the general circulation toward vessel walls, whereas spherical NPs tend to follow the streamlines. (B) Binding avidity. Compared to spherical NPs, NDs have increased particle surface areas in contact with the endothelium, allowing a greater number of targeting ligand interactions to enhance the binding strength.

processes.<sup>69</sup> Overall, oblate shaped NPs (including disc or worm-like NPs) showed improved cellular internalization and favor efficient delivery of therapeutics owing to their large surface areas, multiple attachment points on cells, and reduced clearance by macrophages of the reticuloendothelial organs resulting in prolonged blood circulation half-lives. 63,70-73 Generally, NPs with larger aspect ratios (i.e., non-spherical NPs) are taken up in higher frequency and at faster rates.<sup>27,63</sup> When decorated with targeting ligands, the oblate shape particles form a greater number of multivalent interactions leading to improved cellular uptake even at a high fluid flow rate<sup>74</sup> (Fig. 3B).

In this context, NDs offers many advantages over other nano-formulations due to their uniform ultra-small size, discoidal shape, and site-specific functionalization for cancer signature receptors. Among the other nanocarriers, LIPs offer advantages such as biocompatibility and biodegradability, low toxicity, facile surface functionalization, and possibility of controlled drug release, but they can trigger hypersensitivity reactions and have stability problems. Other organic nanocarriers such as micelles offer similar advantages but are limited to the encapsulation of hydrophobic drugs with relatively low efficiency and suffer from difficulty in scaling up and often unfavorable premature drug release profiles, aggregation, and toxicities. 12,75-77 Inorganic NPs such as mesoporous silica NPs, superparamagnetic iron oxide NPs, carbon nanotubes, gold NPs, metal-organic frameworks, and quantum dots offer some distinct advantages such as large specific surface areas, uniformity in sizes, high stability, facile functionalization, and unique optical, electrochemical, magnetic properties suitable for theranostic applications.<sup>75</sup> However, limitations such as high toxicity, non-biodegradability, accumulation in vital organs, high cost of large-scale production, and particle aggregation restrict many inorganic NPs from translating to clinical applications. 78,79

Although LNDs encased by MSPs or SMALPs have gained increasing popularity in the study of membrane proteins shortly after their discovery in 2000s, 28,33 their uniform, nanoscale and tunable sizes (i.e.,  $\sim 10-20$  nm), large specific surface area, rapid cellular internalization, and high biocompatibility present them as a desirable drug-delivery platform.80 For example, the size of LNDs can be precisely controlled by using suitable MSP constructs, typically ranging from ~10 to

 $\sim 20$  nm. <sup>54,81,82</sup> Compared to spherical NPs, the disc-like structure of conventional LNDs and more recently developed PNDs or HNDs offers many advantages, such as improved circulation half-lives, cellular uptake, biodistribution, and microvascular adhesion. 66,71,83,84 A brief comparison of the pros and cons for each type of ND platform (with respect to cancer diagnosis and mitigation) is provided in Fig. 4. The anisotropy effect can be further enhanced with ligand modification at specific locations on the NDs, including either planes or edge modifications.<sup>27</sup> These properties of NDs are highly merited for the development of novel cancer diagnosis and treatment options that exploit the NDs as carriers for a broad range of imaging probes, chemotherapeutics, vaccines, and anti-cancer genes.53

Besides their well-defined nanoscale sizes and anisotropic shapes, NDs in general have excellent biocompatibility and biodegradability, a highly desirable feature for drug-delivery applications. Since the major component of NDs is either biodegradable lipids (for LNDs and SMALPs) or biodegradable and biocompatible polymers (PNDs), they can be metabolized by enzymes like protease, esterase, metalloproteases etc. Cross linked silicates in the HNDs may produce metabolic resistance and accumulation in the body, but silica is listed amongst the "generally regarded as safe" substances by the Food and Drug Administration (ID Code: 14808-60-7). The buffer incompatibility of conventional SMALPs is a concern, but this problem is solved by the recent development of SMA-like copolymers with unlimited buffer compatibility. 35,85,86

#### 2.1 General methods for the assembly of NDs

The methods for preparing different types of NDs are varied. For example, the LNDs are assembled by mixing an optimal ratio of lipids of choice with suitable MSPs in the presence of an appropriate detergent, followed by removal of detergent below its critical micelle concentration (CMC) by different methods such as dialysis, dilution or using Bio-beads. Finally, the self-assembled LNDs are obtained by suitable affinity column purification;36 For SMALPs assembly, the liposomes and SMA or SMA-like copolymers are incubated in a suitable buffer for varying length of times depending on the nature of the lipids and the copolymers. Once the liposomes are cut by the copolymers into SMALPs, the resultant products are

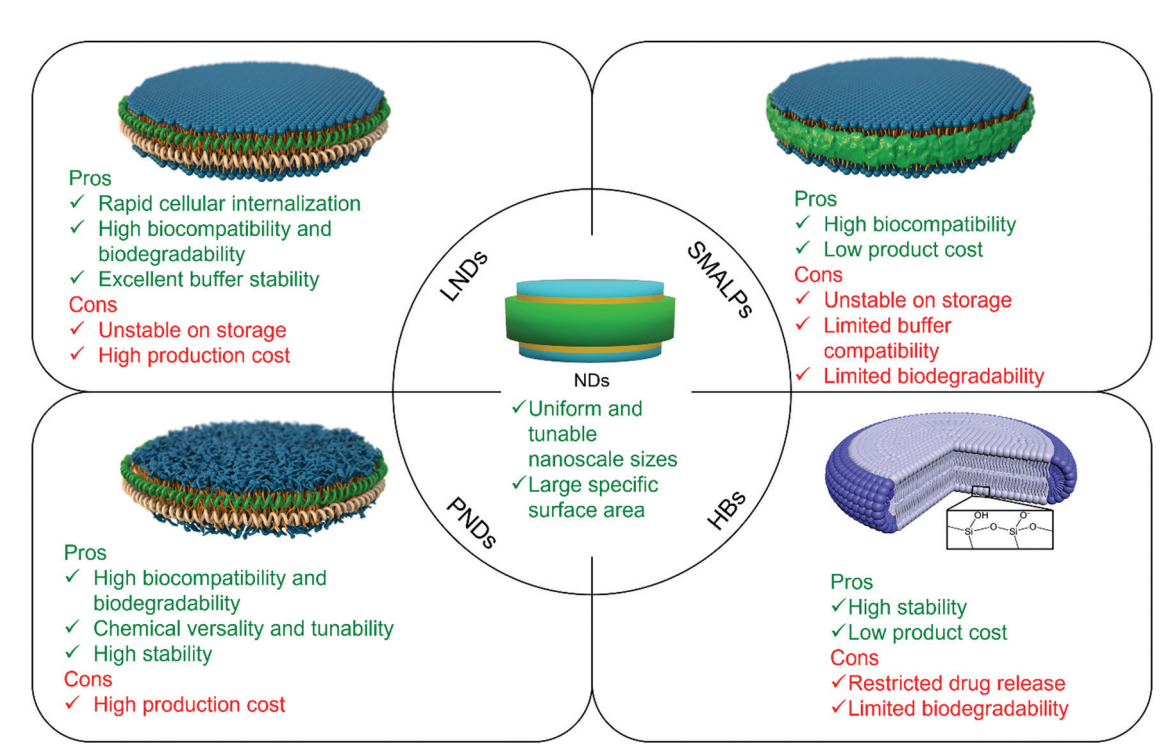


Fig. 4 The merits and limitations of different classes of anticancer NDs. NDs structure reproduced with permissions from ref. 26 Copyright 2020, Frontiers Media S. A. and ref. 27 Copyright 2017, John Wiley and Sons.

generally purified by size-exclusion chromatography; For PNDs assembly, an optimal ratio of polymersomes and MSPs are solubilized in a suitable detergent followed by removal of detergents similarly to the preparation of LNDs. The selfassembled PNDs are collected after purification by the affinity columns;<sup>36</sup> For HBs or HNDs, they are generally prepared by film hydration method. Typically, CFL and short-chain phospholipids at an optimal ratio were dissolved in organic solvent (e.g., CHCl<sub>3</sub>), the solution was subsequently dried to obtain a lipid film. The lipid film was then hydrated with ultrapure water followed by continued hydration overnight.<sup>27</sup> For detailed protocols for the assembly of different NDs, we direct the readers to the research articles and protocols on LNDs,87,88 SMALPS, 35,89 PNDS, 36 and HNDS, 27,90 respectively.

#### 2.2 Stability of NDs

**Review Article** 

Like self-assembled polymersomes, liposomes, or micelles, selfassembled NDs are subjected to disassembly-assembly equilibrium, and the energetics of individual equilibriums depends on the structure and properties of the amphiphiles. Taking the self-assembly of micelles in aqueous solutions for example, when the concentration of amphiphiles increases above its CMC, they start to associate in order to minimize water contact with their hydrophobic moieties. This association favors their hydrophilic regions to make contact with surrounding aqueous solutions while shielding their hydrophobic regions away from water and towards the micelle center.91 By doing so, a hydrogen-bonded network of water molecules that would be otherwise needed to surround the hydrophobic region of individual amphiphiles are also freed and the overall free energy of the system is minimized. 92 Similarly, the self-assembly of NDs is also driven by minimizing the overall free energy of the system, where the amphipathic proteins, synthetic polymers, or short-chain lipids self-assemble to encase individual amphiphilic membrane patches and protect them from exposing their hydrophobic membrane edges to aqueous solutions. The stability of NDs depends on their chemical compositions. For example, just like polymersomes are in general more stable than liposomes, PNDs are more stable than LNDs.

In the following sections, we will discuss the application of various forms of NDs on selective delivery of imaging agents for early cancer detection and chemotherapeutics for cancer treatment. It is important to note that on a few occasions during our discussions, we use high-density lipoproteins (HDLs) and low-density lipoproteins (LDLs) to represent the NDs following the nomenclature frequently used in the original publications, where HDLs/LDLs were used synonymously as NDs because many reported HDLs/LDLs were specified to be discoidal in shape. 51,82,93 It should be pointed out that although HDLs and LDLs frequently assume the ND structures, they could acquire a spherical shape depending on the amount and type of lipids being encased by the apolipoproteins.<sup>24</sup>

# NDs for early cancer detection

Early detection of cancer is one of the paramount requirements for successful treatment and is directly associated with low cancer mortality.94 Cancer imaging, including fluorescent imaging, computed tomography (CT), MRI, transabdominal

or endoscopic ultrasound imaging, and positron emission tomography (PET) imaging are often used for early-stage cancer detection. 95 Among these techniques, CT, MRI, and ultrasound imaging are anatomical imaging modalities. Fluorescent imaging and PET are molecular imaging techniques that complement anatomical imaging modalities by providing functional and molecular information. 96 However, the low number density of early-stage tumor cells often hidden deep in healthy organs and the lack of noticeable signs or symptoms possess major challenges in early cancer detection. In addition, molecular imaging for early-stage small tumors is often inadequate due to non-specific and insufficient accumulation of imaging agents in the tumor cells because of the poor delivery of those imaging agents.

Given that the increased metabolic demand of cancer cells as compared to the healthy cells is met by receptor-mediated access to large quantities of nutrients, cancer cells overexpress specific receptors known as "cancer signatures", such as HER2/ neu, scavenger receptor class B type-1 (SR-B1), epidermal growth factor receptor (EGFR), somatostatin, folic acid receptors (FAR),  $\alpha_{\nu}\beta_{3}$  integrins, and low-density lipoprotein (LDL) receptors. <sup>97</sup> The overexpressed cancer signatures serve as an important tool to selectively target cancer cells for diagnostics and treatment (Fig. 5).

Because of their nanoscale size, discoidal shape, and ease of incorporation of a wide array of imaging agents, NDs have immerged as a powerful tool for the delivery of imaging agents for cancer detection. Generally, the payload can be loaded at three chemically distinct environments of NDs: (1) into the hydrophobic core; (2) onto the shell (or mantle), and (3) on the corona (or crust), depending on the physicochemical properties of the payload and ND design. 51,53 Importantly, by chemically attaching specific tumor ligands either on the planes or edge of

the NDs, the tagged NDs can be routed to target tumor cells selectively.

Besides carrying chemotherapeutics directly with the NDs for their selective delivery to cancer cells, another often used strategies is to modify anticancer drugs into prodrugs and deliver the prodrugs instead.98 There are excellent recent reviews describing the application of prodrugs for cancerspecific targeting, 99-101 and linker-specific prodrugs such as nucleoside-based, 102 disulfides-based, 103 pH-sensitive, 104 reactive oxygen species sensitive prodrugs, 105 and many others.1 Prodrug strategy uses chemical functional groups such as esters (such as carboxyl, carbamate, carbonate, phosphate, or sulfate esters), amide, oxime, imine, disulfide, or thioethers groups between the drug and the promoiety/nanocarrier system. The promoiety attached with the drug plays a key role in overcoming various barriers, enhancing drug targeting, and improve drug-like properties. The conjugation of the drug and the prodrug moiety should be stable till it reaches the target site; however, once it reaches the target site, a fast drug release is expected to show the desired therapeutic effect. The release process is likely to take place in the TME either in response to a specific trigger such as elevated levels of cellular enzymes (e.g. esterases, phosphateses, sulphatases, matrix metalloproteases, thymidine phosphorylase, endopeptidase, cathensin B, etc.), 1,100 elevated levels of reactive oxygen species, low pH, 103 or specific ligand-receptor interaction or in response to external stimuli such as thermal, 106 ultrasound, 107 light 108 or magnetic.109

#### 3.1 Targeted delivery of fluorescent imaging agents

3.1.1 SR-B1 receptor mediated delivery of imaging agents. The overexpression of SR-B1 receptors in some cancers (such as

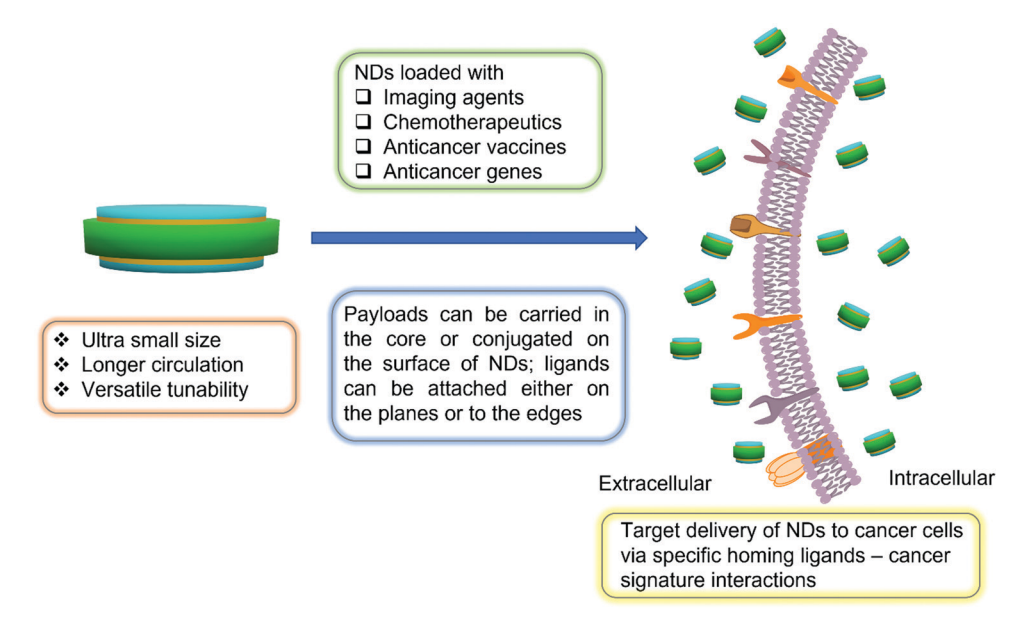


Fig. 5 Early detection and elimination of cancer cells enabled by ND platforms that target cancer signatures. NDs offer several advantages over other nanoparticles, such as well-defined sizes, long circulation time, high cellular uptake, and versatile surface functionalization options. A variety of diagnostic and/or therapeutic agents can be loaded either in the core or conjugated on the surface of NDs. Integration of homing ligands that target specific cancer signatures with NDs results in the highly efficient delivery of payloads into cancer cells.

**Review Article** Chem Soc Rev

prostate, breast, and ovarian cancers 110) facilitates the selective transport of cholesterol esters from HDL to the cytosol through a hydrophobic channel in the cell membrane. 111 Using the SR-B1 receptors route, Zhang et al. reported that a HDL mimicking nanocarrier system can be assembled using apoA-1 mimetic peptide (FAEKFKEAVKDYFAKFWD) and loaded with a lipid-anchored near-infrared imaging dye, 1,1'-dioctadecyl-3,3,3',3'-tetramethylindotricarbocyanine iodide bisoleate (DiR-BOA). The DiR-BOA loaded nanocarriers are spherical, whereas empty nanocarriers have a discoidal shape with a diameter of  $\sim$  16 nm. It was shown that Chinese hamster ovary cells having high expression of SR-B1 exhibited 55 times higher internalization and fluorescein signal from DiR-BOA loaded nanocarriers. In a mouse model, KB tumors (SR-B1<sup>+</sup>) showed a 3.8-fold higher fluorescence signal compared to HT1080 tumors (SR-B1<sup>-</sup>). 111 Cao et al. also reported that another fluorescent imaging agent, Bacteriochlorin e6 bisoleate (Bchl-BOA), loaded in HDL (HDL-Bchl-BOA) had an average diameter of ~12 nm. Each HDL-Bchl-BOA had an average of 2-3 molecules of apoA-1 and 6-9 molecules of Bchl-BOA. HDL-Bchl-BOA was preferentially taken up by Chinese hamster ovary cells (SR-B1<sup>+</sup>), resulting in a high fluorescence signal in KB cells in the athymic nude mice model. 112 Similarly, NDs of pyropheophorbide-conjugated with 1-palmitoyl-2-hydroxy-sn-glycero-3-phosphocholine (pyro-lipid) were developed by Ng et al. The pyro-LNDs had a mean diameter of 10-30 nm with an elliptical structure. The pyro-LNDs were internalized and showed high fluorescence in Chinese hamster ovary cells stably transfected with SR-B1<sup>+</sup>. 113

The effects of size, shape, and pegylation on tumor targeting were studied by Tang et al.114 They developed synthetic HDLs (sHDL) and their pegylated counterparts (PEG-sHDL), and compared the tumor-targeting efficiencies of those NDs with LIP and pegylated LIP (PEG-LIP). The particle sizes of spherical LIP and PEG-LIP were  $\sim 130$  and  $\sim 100$  nm, respectively, whereas the discoidal sHDL and PEG-sHDL showed average diameters of  $\sim 9.5$  and  $\sim 12$  nm, respectively. The efficient cellular uptake (in BHK-SR-B1 and HCT 116 colon carcinoma cells), tumor spheroids penetration, tumor accumulation, and

in vivo distribution of all the NPs was monitored by loading 3,3dioctadecyloxacarbocyanine perchlorate (DIO) or 1,1'-dioctadecyl-3,3,3',3'-tetramethylindotricarbocyanine iodide (DiR) as a model drug and tracer. It was shown that sHDL, which targets the SR-B1 receptor, has significantly higher tumor targeting, penetration, and accumulation than LIP, PEG-LIP, and PEGsHDL<sup>114</sup> as shown in Fig. 6A.

3.1.2 FAR mediated delivery of imaging agents. FARs are extensively expressed on epithelial malignancies such as ovarian, breast, colorectal, cervical, and nasopharyngeal cancers. 117 Covalently linked folic acid (FA) with macromolecules retains its high affinity for FARs and this approach to homing the tumor has been investigated extensively. 118 The conjugation of FA to the NDs can be achieved either to apoA-1 protein (or similar proteins) or a long chain lipid anchor that may be inserted in both planes of the NDs. Using this strategy, Zhang et al. conjugated FA with highly basic lysine residues of apolipoprotein B (ApoB)-100, which required a minimum of  $\sim$  50% lysine residue modification to abolish uptake of LDL by the low-density lipoprotein receptors and to direct them to the FRs. Compared with native LDL ( $\sim 20$  nm), the average particle diameter of FA modified LDL increased to ~26 nm when loaded with 1,1'-dioctadecyl-3,3,3',3'-tetramethylindocarbocyanine (Dil) (DiI-LDL-FA) and ~24 nm when loaded with tetra-t-butyl-silicon phthalocyanine bisoleate. FA modified LDLs effectively deliver DiI, loaded on the surface or tetra-tbutyl-silicon phthalocyanine bisoleate core loaded dye. Both DiI-LDL-FA and reconstituted tetra-t-butyl-silicon phthalocyanine bisoleate folate-conjugated LDL (r-Pc-LDL-FA) were selectively taken up by FR<sup>+</sup> KB and HepG2 (LDLR<sup>+</sup>) cells. This uptake was blocked by the addition of free FA.97 Using a similar strategy, Corbin et al. developed engineered HDLs to load the fluorescent dye DiR-BOA. The engineered HDL had a mean diameter of  $\sim 9.0$  nm and has approximately two molecules of DiR-BOA (core loaded) and 19 FA molecules attached to lysine residues of apoA-1. These particles accumulated selectively in FR<sup>+</sup> KB cells in vitro and FR<sup>+</sup> KB cell-derived tumors. 119 In another strategy, Corbin et al. conjugated FA to apoA-1 after

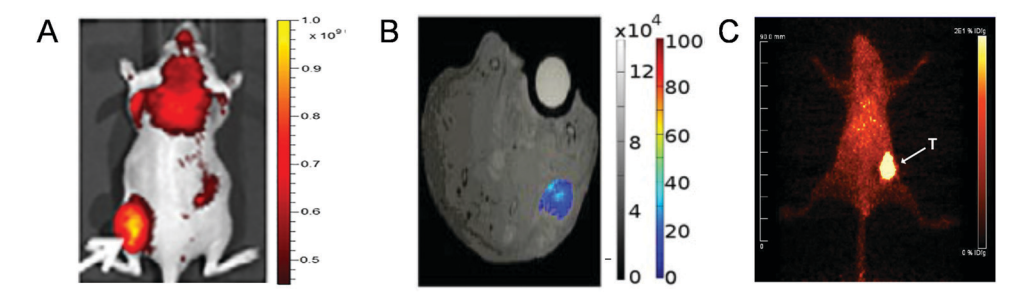


Fig. 6 Examples of ND platforms used for early cancer detection. (A) The in vivo fluorescence imaging of HCT 116 tumor-bearing nude mice 72 h after administration of DIO loaded sHDL.<sup>114</sup> Tumors were located in the left flanks as indicated by the arrows, (B) representative in vivo T1-weighted MR images of Swiss nude mice bearing subcutaneous human EW7 Ewing's sarcoma tumors 24 h post-injection of reconstituted-rHDL (rHDL) loaded with amphiphilic Gd chelates. 115 Enhanced pixels within the tumors were color-coded. Gray scale represents signal intensity; color scale represents the percentage of enhanced pixels above a threshold that is defined by the mean intensity of the whole tumor and noise of precontrast MR scanning, and (C) PET imaging of CEA positive tumors in CEA transgenic mice bearing CEA/E0771 cells in their right mammary fat pads with 64Cu-DOTA-Antibody injected with 40 μCi of <sup>64</sup>Cu-DOTA-antibody and imaged after 46 h.<sup>116</sup> Reproduced with the permission from ref. 114. Copyright 2017, Elsevier Ltd., ref. 115, Copyright 2010, John Wiley and Sons, and from ref. 116. Copyright 2020, American Chemical Society.

reconstitution of HDLs (rHDLs) preloaded with DiR-BOA. The rHDL(DiR-BOA) had a diameter of  $\sim\!15$  nm with four molecules of DiR-BOA and 44 molecules of FA on each particle. The FA-rHDL(DiR-BOA) was selectively internalized by FA-over-expressed IC5-MOSEC cell lines whereas, rHDL(DiR-BOA) was selectively taken up by SR-B1 $^+$  overexpressing (LdlA[mSR-B1]) cells and SR-B1 $^+$  tumor in mice model. The FA moieties on the surface of the rHDL(DiR-BOA) facilitates the uptake of the NPs into the IC5-MOSEC cells as confirmed by competitive uptake inhibition by adding excess of free FA.  $^{120}$ 

Alternatively, FA can be conjugated to a lipid anchor and adsorbed in both planes of the NDs. In one such example, Tahmasbi Rad *et al.* used folate poly(ethylene glycol)-conjugated distearoyl phosphoethanolamine (DSPE-PEG<sub>2000</sub> folate) to construct the NDs and loaded them with Nile Red or *meta*-tetra(hydroxyphenyl) chlorin for photodynamic therapy. A morphology comparison between LND and LIP (with identical chemical composition) was performed where the NDs had a hydrodynamic radius of 10–12 nm, whereas nanovesicles had 27–30 nm. In FR-overexpressed KB cells, a higher cellular uptake and high fluorescence intensity were observed in meta-tetra(hydroxyphenyl) chlorin-loaded NDs irrespective of conjugation of FA compared to similar vesicles. Similarly, KB tumor-bearing mice showed higher uptake and tumor penetration rate of FA-NDs compared to FA-vesicles.<sup>121</sup>

3.1.3 EGFR mediated delivery of imaging agents. EGFR are cell surface receptors and overexpressed in various solid tumors, including cancers of the brain, breast, colon, head, and neck, lung, ovary, and pancreas. Langet al. developed HDL-mimetic NPs using apoA-1 mimetic peptide (FAEKF-KEAVKDYFAKFWD) and decorated with DSPE-PEG\_2000-EGF. The fluorescent NPs carry  $\sim 50$  molecules of DiR-BOA with a diameter of  $\sim 15$  nm. The functionalization of NPs with EGF ligand has minimal effect on particle size and showed almost two folds higher accumulation in EGFR-GFP-IdIA7 and KB cells (EGFR $^+$ ). These NPs selectively accumulated in a xenograft KB cells tumor model (EGFR $^+$ ) and showed 2.5-fold higher accumulation compared to EGFR $^-$  tumors. Lange in various solid

### 3.2 Delivery of MRI contrast agents using NDs

The optical imaging for early cancer detection has problems such as limited penetration depth and lack of anatomical definition. Thus, other high-resolution techniques are required for imaging deep-seated tumors for molecular details. MRI offers high spatial resolution with anatomical details and excellent contrast. Gadolinium was shown as a highly efficient MRI agent co-delivered with a fluorescent dye (DiR) or 1,2dimyristoyl-sn-glycero-3-phosphoethanolamine-N-(lissamine rhodamine B sulfonyl) using the ND platform by Chen et al. for cancer imaging. To target angiogenic endothelial tumor cells, the Gadolinium and dye-loaded rHDL were decorated with  $\alpha_v \beta_3$ -integrin-specific cyclic 5-mer RGD peptide. The rHDL-RGD NP loaded with DiR dye had a mean diameter of ~12 nm. Similar to the in vitro cellular uptake, the rHDL-RGD NPs had high tumor targeting efficiency in the human sarcoma xenograft model for deep-seated tumors and provided high sensitivity and anatomical resolution as shown in Fig. 6B. 115

#### 3.3 Delivery of PET imaging agents using the NDs platform

PET uses small amounts of radioactive materials to evaluate organ and tissue functions at the molecular level. By identifying changes at the cellular level, PET can detect the early onset of disease. Among some popular radioactive agents, <sup>64</sup>Cu is an attractive radionuclide due to its relatively long half-life (12.7 hours) and low maximum positron energy (0.66 MeV). Delivery of radioactive materials required special functional modality on the nanocarriers systems to make a complex with radioactive material such as DOTA. One of the strategies applied by Huda et al. was to functionalize the lysine groups of α-helices of the scaffold protein MSP1E3D1 with DOTA to reconstitute 64Cu labeled NDs. Conjugation of DOTA to the MSP had minimal effect on its amphipathic folding and ability to form NDs. Each NDs has an average of 5 DOTA per MSP with an average diameter of ND  $\sim$  13 nm with discoidal shape. In the human lung carcinoid tumor model, the 64Cu bearing NDs showed a steady increase of NDs concentration in tumors as visualized by PET and computed tomography (CT) images. 124

Recently, Wong *et al.* used a different approach for the delivery of <sup>64</sup>Cu using NDs where a lipid anchor was conjugated with DOTA for insertion on both planes of the NDs. Also, the tumor-targeting efficiency was enhanced by attaching carcinoembryonic antibody (CEA) to the surface of NDs. The anti-CEA antibody conjugated NDs had a diameter of 13–14 nm. In CEA-positive tumors in CEA transgenic mice, the antibody fragment fails to direct the NDs to the tumor, whereas attachment of intact anti-CEA antibody to the NDs provided the high tumor uptake of 40% ID/g (Fig. 6C and 7C).<sup>116</sup>

In another study, Pérez-Medina *et al.* used <sup>89</sup>Zr as PET agent incorporated in reconstituted HDLs (rHDLs) to image tumorassociated macrophages in the breast cancer mice model. The long-lived positron-emitting nuclide <sup>89</sup>Zr was incorporated in the NDs either by conjugating through phospholipid or apoA-1 to generate <sup>89</sup>Zr-PL-HDL or <sup>89</sup>Zr-AI-HDL. Both NDs were discoidal in shape with an average diameter of  $\sim$ 8.0 nm. Both types of NDs resulted in high tumor accumulation of radioactive material and good colocalization in tumor-associated macrophage-rich areas in tumor sections. <sup>128</sup>

### 3.4 Delivery of inorganic NPs as imaging agents by NDs

Inorganic NPs such as gold or iron oxide NPs have distinct advantages for *in vivo* imaging. Gold NPs have a high X-ray attenuation in CT,  $^{129}$  iron oxide NPs offer good contrast for MRI,  $^{130}$  whereas quantum dots offer narrow and well-defined fluorescence emission peaks without photobleaching effects.  $^{131}$  These inorganic NPs can be attached to hydrophobic nanostructures that can be loaded in the core of NDs. The HDLs loaded with modified inorganic nanocrystals in the core are spherical with a diameter of  $\sim 10$  nm while retaining all biological features of HDL. Such chemically modified iron oxide,  $^{132}$  gold,  $^{132,133}$  and quantum dot-loaded HDL  $^{132,134}$  were used for MRI, CT, and optical imaging, respectively for detection of

**Review Article** 

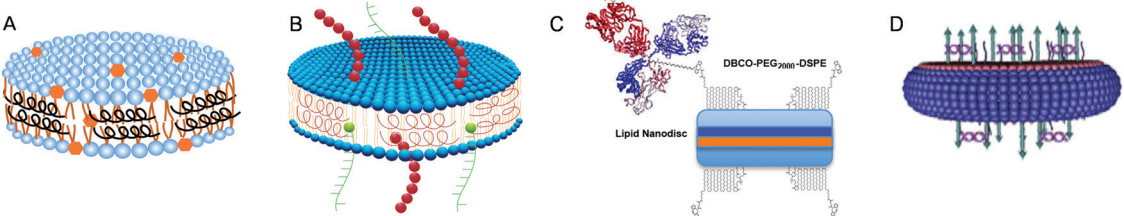


Fig. 7 Examples of different strategies that exploit NDs as carriers for cancer mitigation. (A) Hydrophobic WGA-TA (orange hexagonals) loading in the lipid core (blue dots with orange tails) of the NDs reconstituted by peptide 22A (black coils), 125 (B) NDs for delivery of cysteine-modified antigen (Ag) peptides (maroon filled circles as chains) and cholesterol-modified immunostimulatory molecules (Cho-CpG, green chains) inserted in LNDs, <sup>1</sup> (C) delivery of full-length anti-CEA antibody using NDs modified with doping of DSPE-PEG<sub>2000</sub>-DBCO, <sup>116</sup> and (D) delivery of cancer therapeutic genes (siRNA) using NDs technology, where siSTAT3 (purple helix) was complexed with DOTAP (purple lines) and loaded on the NDs doped with DSPE-PEG<sub>2000</sub> - cRGD (green arrows). The HNDs were prepared from CFL (maroon filled circles) and 1,2-dihexanoyl-sn-glycero-3-phosphocholine (blue filled circles); both plane and edge loaded siSTAT3 NDs were synthesized. 127 Reproduced with the permission from ref. 125. Copyright 2017, Dove Press, ref. 126. Copyright 2017, Nature Publishing Group, ref. 116. Copyright 2020, American Chemical Society, and ref. 127. Copyright 2020, Elsevier Ltd.

atherosclerosis. These nanostructures are desirable platforms for cancer imaging; however, their efficiency for cancer imaging has not been explored yet.

# 4. NDs for anticancer drug delivery

Cancer is a pathophysiologically heterogeneous disease that needs varied strategies for effective control. The most popular strategies include surgery, radiation therapy, chemotherapy, and immunotherapy. 135 With an advanced understanding of molecular mechanisms in TME, novel anticancer drugs have been continuously discovered, which include small molecules, oligonucleotides, plasmid DNAs, siRNAs or miRNAs, antibodies, and engineered immune cells capable to control the specific protein or signaling pathways that are aberrantly expressed in the TME. 1,136

NDs have been extensively explored for drug delivery to cancer cells by utilizing the benefits of their small size and anisotropic geometry for enhanced cellular internalization. Different strategies such as physisorption, conjugation, or prodrug approaches have been explored to carry a variety of payloads by NDs. In the following sections, we will discuss the use of NDs for the delivery of chemotherapeutics, photosensitizers, chemoimmunotherapeutics, cancer vaccines, and anticancer genes for cancer mitigation.

#### 4.1 Delivery of chemotherapeutics

Despite the significant advancements in cancer therapy, cancer remains the second leading cause of death globally.137 Chemotherapy for cancer mitigation started after the use of nitrogen mustard during World War II. After this discovery, hundreds of cancer chemotherapeutic drugs have been developed. 138,139 However, chemotherapy frequently fails in cancer treatments due to poor pharmacokinetics and wide distribution of drugs in vivo, insufficient delivery, and multiple drug resistance.140 Various strategies have been explored to load hydrophobic drugs and hydrophilic peptides in the NDs and successfully deliver these payloads to cancer cells.

Loading a hydrophobic drug into the lipid core of NDs using hydrophobic and electrostatic interactions is a common approach where degradation of the apoA-1 or apoA-1 mimetic peptide by protease results in disassembly of the NDs and subsequent drug release. For example, McConathy et al. have developed rHDL particles loaded with PTX that were assembled using apoA-1 with an incorporation efficiency of  $\sim 50\%$  of the initial drug load. The PTX loaded rHDL showed improved cytotoxicity against several cancer cell lines (5 to 20 times) when compared to the free drug. More importantly, the PTX loaded rHDL were well tolerated by mice and showed significantly low toxicity compared to free PTX. The higher cellular uptake mechanism of PTX loaded rHDL showed SR-B1 mediated internalization in SR-B1-transfected ldl A7 and in PC3 cells. 141 These rHDLs, when functionalized with FA via apoA-1 modification, were rerouted to the FR overexpressed cells (OVCAR-3 cells). 142 Similar to the natural HDL development process, the engineered discoidal HDLs become spherical by the action of the lecithin-cholesterol acyltransferase. Such maturation can affect the loaded drugs in the NDs. The effect of lecithin-cholesterol acyltransferase on discoidal PTX loaded HDL, PTX (P-d-rHDLs) was studied by Jia et al. and showed that re-modeling of the NDs to a spherical shape, increasing their diameter from  $\sim 68$  nm to  $\sim 83$  nm, enhances drug leakage, reduces cellular uptake in vitro, and reduces the cytotoxicity of P-d-rHDLs by ~3 times compared to the non-lecithincholesterol acyltransferase treated group in MCF-7 cells. 143

TAT peptide (YGRKKRRQRRR) is capable of traversing the plasma membrane and induces apoptosis in cancer cells. 144 A genetically fused TAT peptide to a truncated apoA-1 protein was developed by Murakami et al. resulting in a mutant apoA-1 (ΔapoA-1) that overt its recognition from SR-B1. The mutant  $\Delta$ apoA-1 and  $\Delta$ apoA-1-TAT used to form the corresponding DOX-rΔHDL and DOX-rΔHDL-TAT by loading DOX into the lipid core. The empty NDs had a mean diameter of  $\sim$  18 nm for rΔHDL-TAT and rΔHDL, whereas DOX loaded DOX-rΔHDL-TAT had a mean diameter of ~24 nm and DOX-rΔHDL had a diameter of ~155 nm with a DOX loading of ~10% for both NDs. The DOX delivery efficiency of DOX-rΔHDL-TAT was

approximately two times higher than that of DOX-rΔHDL in NCI-H460 cells and A549 cells. Also, the DOX-rDHDL-TAT showed higher anti-tumor activity in the mice tumor model. 145 In a different approach, PEG-stabilized bilayer NDs loaded with DOX (DOX-Disks) were developed by Zhang et al. These NDs had a mean diameter of  $\sim 80$  nm, and high encapsulation efficiency of 96% for DOX, with a pH-sensitive release. The DOX-disks showed long-circulating times in rat blood compared to DOX in solution and showed ~10-fold higher tumor accumulation with lower heart toxicity. The DOX-disks were likely to be internalized in the cancer cells via energy-dependent endocytosis processes, like clathrin-mediated, macropinocytosis-mediated, and non-clathrinand non-caveolae-mediated endocytosis pathways. 146

The apoA-1 mutant, apoA-1<sub>Milano</sub> (apoA-1<sub>M</sub>) was used by Zhang et al. to construct 10-hydroxycamptothecin (HCPT) loaded reconstituted HDL (rHDL<sub>M</sub>-HCPT) with a drug loading capacity of  $\sim 4\%$  (w/w) and a diameter of  $\sim 22$  nm. HCPT was slowly released from rHDL<sub>M</sub>-HCPT and had 70 times improved cytotoxicity compared to the free drug, whereas conventional LIP and rHDLwt-HCPT displayed 27- and 58-times enhanced cytotoxicity, respectively, at an equal dose in SKOV-3 cells. This improved cytotoxicity is likely due to the improved receptorspecific binding of apoA-1<sub>M</sub> to the SR-B1 receptors. The improved receptor-specific binding was also observed in organ-specific delivery of HCPT as a significant increase in drug concentration was observed in almost all tissues except the heart and brain when compared to free HCPT treatment.147

Similarly, HCPT loaded lipid HDL were constructed by Yuan et al. using apoA-1 mimetic amphipathic helix peptide 5A (DWLKAFYDKVAEKLKEAF-P-DWAKAAYDKAAEKAKEAA) for drug delivery to SR-B1 overexpressed colon carcinoma. The HDLs had a discoidal shape with a diameter of  $\sim 10$  nm. The incorporation of HCPT in HDL provided metabolic stability to HCPT and improved 3-fold cytotoxicity in colon HT29 carcinoma cells. The HCPT loaded HDL showed higher serum concentration-time curve (AUC $_{0-t}$ ) and  $C_{max}$  for HCPT-HDL relative to the free HCPT after intravenous administration in rats.148

Ghosh et al. formulated curcumin loaded NDs with an average diameter of ~50 nm and solubilization efficiency of 70%. The curcumin-loaded NDs were significantly more effective in inducing apoptosis than the free curcumin. 149 Further, a detailed mechanistic study of curcumin loaded NDs showed that the apoptosis induction is a result of enhanced generation of reactive oxygen species along with decreased expression of proteins that include cyclin D1, pAkt, pIκBα, and Bcl<sub>2</sub> and enhanced FoxO3a and p27 expression as well as caspase-9,-3, and poly(ADP-ribose) polymerase cleavage. All these effects led to enhanced G1 arrest in MCL cells. 150

Naturally occurring 4,19,27-triacetyl with alongolide A (WGA-TA) isolated from Solanaceae family of plants is a potent antitumor compound. Its low solubility in plasma and short circulation half-life ( $\sim 1$  h) was improved by formulating WGA-TA in sHDL. WGA-TA loaded sHDL (Fig. 7A) were composed the apoA-1 mimetic peptide 22A and had a diameter of 10-12 nm. The WGA-TA loaded-sHDL selectively accumulated

in SR-B1 positive neuroblastoma (NB), 151 adrenocortical carcinoma,125 and triple-negative breast cancer mice models and produced tumor regression. 152

Melittin is a large peptide isolated from European bee venom with high potential as an anticancer agent. 153 Its severe hemolytic effects were addressed by developing melittin-loaded NDs. The flat circular lipid bilayer has a diameter of  $\sim 50$  nm in diameter, surrounded and stabilized by PEG-lipids on the rim, and functionalized with c(RGDyK) to target overexpressed ανβ3 and  $\alpha_v \beta_5$  integrins. The NDs protected melittin against trypsin digestion and prevent hemolysis when injected in mice. The NDs provided higher cellular internalization, improved cytotoxicity, and enhanced tumor regression in integrin overexpressed U87 tumor cells. 154

The effect of drug loading on the stability of very-low-density lipoprotein (VLDL), LDL, and HDL was studied by Kader et al. by loading 5-fluorouracil (5-FU), 5-iododeoxyuridine (IUdR), DOX, and vindesine. The broad molecular weight and large hydrophobic variation among these drugs have a significant effect on drug loading. The relative loading efficiency was vindesine > IudR > DOX > 5-FU among all three classes of lipoproteins. The drug loading did not significantly affect size, morphology, thermal transition temperature  $T_{\rm m}$ , or transition enthalpy  $\Delta H$  of the lipoprotein core compared to the native particles. However, the  $\Delta H$  for LDL-DOX and LDL-vindesine complexes were lower compared to the native particles due to drug immiscibility in the LDL core lipids. The drugs loaded in LDL and HDL were more cytotoxic than the free drug for MCF-7 cells, whereas VLDL-drug complexes had the same cytotoxicity as free drugs. 155

In another study, Subramanian et al. evaluated the combination of cytotoxic drugs loaded in HDLs to synergize the effect of cholesterol-free HDLs. The cholesterol-free sHDL was formulated using peptide 22A and loading the standard regimen of cisplatin, etoposide, DOX or mitotane used for adrenocortical carcinoma chemotherapy. The cisplatin, etoposide, and mitotane had a synergistic effect with cholesterol-free sHDL, whereas DOX acted as an antagonist in NCI-H295R and SW13 cells. This synergistic effect was also observed in improved clonogenic inhibition, increased adrenocortical carcinoma cells apoptosis, and decreased mitochondria membrane potential compared with monotherapy. 156

#### 4.2 Delivery of photodynamic therapeutics

Photodynamic therapy (PDT) is one of the safest and novel noninvasive treatments for various forms of cancer, including cutaneous T cell lymphoma, colorectal cancer, melanoma, and breast cancer. 157,158 PDT uses a nontoxic drug that is activated by irradiation, which causes the generation of cytotoxic reactive oxygen species, particularly singlet oxygen (1O2) that kills the cancer cells. 159 For high therapeutic benefits and minimal toxic effects, a high accumulation of PDT drug in the cancer cell is required. PDT agents were successfully delivered using the ND platform. For example, Ge et al. have developed LNDs loaded with the photodynamic therapy agent hypocrellin B that were constructed using MSP expressed and purified from

**Review Article** Chem Soc Rev

E. coli. The hypocrellin B-ND was discoidal in shape with a diameter of  $\sim$  11 nm and loading efficiency of  $\sim$  40%. The lipid environment of the NDs had no detrimental effect on the light absorption and its potential to generate reactive oxygen species. The hypocrellin B-ND displayed enhanced internalized in MCF-7 cells and proved more cytotoxic upon exposure to light compared to cells treated in the dark. 160

### 4.3 Delivery of chemoimmunotherapeutics

Cancer immunotherapy proved successful in achieving longterm survival in 10-30% of cancer patients; however, immune therapy utilizing immune checkpoint blockers is ineffective in most cases<sup>161</sup> because the therapeutic efficacy largely depends on pre-existing anti-tumor T-cells. Thus, most tumors where a low population of tumor-specific T-cells are available did not provide the desired therapeutic output. 162 To improve the abundance of anti-tumor T-cells, immunotherapy is combined with therapeutic vaccines, 163 radiation therapy, 164 and chemotherapy<sup>165</sup> for strong anti-tumor immunity. Among chemotherapeutics, DOX and PTX can activate anti-tumor T-cell responses through a special form of tumor-cell killing known as immunogenic cell death. 166 Tumor cells undergoing immunogenic cell death up-regulate the expression of calreticulin and highmobility group box 1, which are "eat me" and "danger" signals, respectively, and produce triggered antigen-specific T-cell responses. 167 Delivery of DOX to stimulate the immune system using a synthetic HDL has proved beneficial (Fig. 8).

The sHDL developed by Kuai et al. were composed of the apoA-1 mimetic peptide 37A and DOX was incorporated in the sHDLs by conjugation with 1,2-dipalmitoyl-sn-glycero-3-phosphothioethanol through N-b-maleimidopropionic acid hydrazide for pH-sensitive release in the TME. The DOX-loaded sHDL (sHDL-DOX) has a loading efficiency of  $\sim 2\%$  with a diameter of  $\sim$  10 nm. The sHDL-DOX showed enhanced tumor accumulation and triggered robust expression of danger signals associated with immunogenic cell death within tumors and generated potent anti-tumor T cell responses. The sHDL-DOX treatment broadens the T-cell mediated epitope recognition for tumor-associated antigens (CT26 gp70 (AH1) (H-2L<sup>d</sup>-restricted SPSYVYHQF)), neoantigens (Adpgk protein), and the intact whole tumor cells (CT26 tumor cells). The co-treatment of sHDL-DOX with αPD-1 (IgG antibody) induced complete regression of established colon carcinoma in 80-88% mice and provide 100% protection among all survivor mice when re-challenged with tumor cells. 168

In another example, Kadiyala et al. loaded DTX in LNDs to treat glioblastoma by the chemoimmunotherapy approach. To enhance the immune response, NDs were loaded with the Toll-like receptor-9 agonist CpG oligodeoxynucleotide through its conjugation with cholesterol. The DTX loaded sHDL NDs (DTX-sHDL) were assembled using 22A peptide and had a diameter of ~10 nm and a discoidal shape. The DTX-sHDL-CpG treatment resulted in tumor cell death with concomitant release of the damage-associated molecular pattern molecules calreticulin and high-mobility group box 1 into the TME in glioblastoma bearing mice. Release of CpG from the NDs activates macrophages and dendritic cells resulting in simultaneous

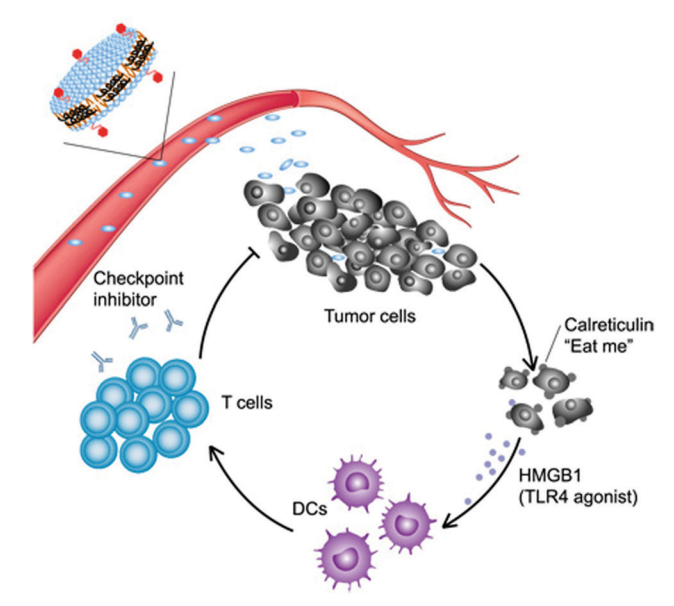


Fig. 8 NDs as nanocarriers for the delivery of chemoimmunotherapeutics. The sHDL enables intratumoral delivery of DOX followed by internalization and pH-responsive release of DOX in the endosomes/ lysosomes. Released DOX kills tumor cells and triggers ICD, promoting up-regulation of CRT (the "eat me" signal) and release of danger signals such as HMGB1. DCs recruited to the immunogenically dying tumor cells phagocytose them, process tumor antigens, and cross-prime tumor antigen-specific T cells. Antitumor immunity primed with sHDL-DOX synergizes with immune checkpoint blockade, leading to efficient elimination of established tumors and prevention of tumor relapse. 168 Reproduced with the permission from ref. 168. Copyright 2018, American Association for the Advancement of Science.

uptake and processing of tumor antigens. The activated dendritic cells migrate to the draining lymph nodes, presenting tumor antigens to CD8 T cells resulting in anti-tumor CD8<sup>+</sup> T-cellmediated immunity. The therapeutic efficiency of DTX-sHDL-CpG was further enhanced by combination with radiation therapy, leading to tumor elimination from 80% of the glioblastoma bearing animals. More importantly, the immunotherapy developed a long-term immunological memory, providing 100% mice survival after tumor rechallenging without any further treatment.169

#### 4.4 Delivery of cancer vaccines

Peptide-based cancer vaccines are rapidly gaining popularity owing to their excellent safety profile, ease of manufacturing, and quality control. However, peptide-based vaccines have frustrating weak immunogenicity and generally require co-delivery of immunological adjuvants for potent immune response.<sup>170</sup> For example, delivering peptide-based vaccines to the draining lymph nodes is challenging and subsequently leads to immunological tolerance and cytotoxic T lymphocytes fratricide.171 Recently, Kuai et al. developed sHDL to deliver peptide-based cancer antigen mixed with adjuvants and tumorspecific mutant neoepitopes. ApoA-1-mimetic peptide 22A was used for lipid solubilization and intracellular release of Ag from the sHDL was controlled by a reduction-sensitive conjugation

(disulfide linkage) between the Ag and sHDL. The sHDL NDs were loaded with Ag peptides, OVA<sub>257-264</sub> (a model CD8α<sup>+</sup> T-cell epitope Ag from ovalbumin), and Adgpk (neoantigen in MC-38). The final NDs co-loaded with Ag and CpG (Fig. 7B) had  $\sim 6.5$  Ag peptides and ~1 CpG molecule per NDs, with discoidal morphology and diameter of ~10 nm. The sHDL markedly promoted the delivery of Ag/CpG to the Delphian lymph nodes and induced CD8\alpha^+ T-cell responses. Notably, the sHDL-Ag/CpG induced a peak frequency of  $\sim 21\%$  Ag-specific CD8 $\alpha^+$  T cells and Ag-specific cytotoxic T lymphocytes responses after the third vaccination, whereas the mixture of free Ag peptides (SIINFEKL or CSSSIINFEKL) and CpG induced 1-3% Ag-specific cytotoxic T lymphocytes. When mice immunized with sHDL-Ag/CpG were challenged with B16OVA cells there was no detectable tumor for up to 28 days and there was no toxicity. In contrast, mice vaccinated with free Ag peptides + CpG or Ag + CpG + the immunoadjuvant Montanide succumbed to tumors with marginal survival benefits. A combination of sHDL-Adpgk/CpG with anti-PD-1 treatment generated robust neoantigen-specific cytotoxic T lymphocytes responses with complete tumor regression in most mice and 100% survival of mice after rechallenging with cancer cells. The strong anti-tumor T-cell responses produced by the NDs in combination with immune checkpoint inhibitors showed the remarkable potential to eliminate tumors in >85% of animals<sup>126</sup> (Fig. 9).

Recombinant proteins and peptide antigen-based vaccines have low immunogenicity and necessitate the administration of

immune-stimulating adjuvants such as toll-like receptor agonists (TLR agonists) to promote the immune response. Recently, Kuai et al. developed sHDL loaded with monophosphoryl lipid A (MPLA, a TLR4 agonist), CpG-rich oligonucleotide (CpG, a TLR9 agonist), and the antigen protein ovalbumin, or the E7 antigen peptide that produces strong humoral immune responses in animal models. The adjuvant-loaded NDs had an average diameter of  $\sim 10$  nm and an encapsulation efficiency >80% for MPLA and >95% for cholesterol-CpG. The NDs co-loaded with dual adjuvants (ND-MPLA/CpG) effectively activated dendritic cells when compared with free dual adjuvants or even NDs containing either MPLA or CpG. The ND-MPLA/CpG admixed with ovalbumin significantly improved antigen-specific CD8<sup>+</sup> T cell responses in B16F10-OVA tumor-bearing mice, inducing regression of established melanoma tumors. Similarly, when TC-1 tumors in mice were treated with ND-MPLA/CpG admixed with E7 antigen peptide, ~20% E7specific antigen-specific CD8+ T cells were produced, leading to potent anti-tumor efficacy against established TC-1 tumors. 172

In general NP-based vaccines are administered via the subcutaneous (SC) route, whereas the conventional vaccines by the intramuscular route, presumably due to the "depot" effect for prolonged vaccine delivery. Recently, sHDL based vaccines loaded with CpG and neoantigen Adpgk (sHDL-Adpgk/CpG) along with the immune checkpoint blockers anti-PD-1 and anti-CTLA-4 IgG antibodies, significantly enhanced NP delivery by the SC route to draining lymph nodes. The SC route improved NDs uptake by antigen-presenting cells and generated a 7-fold

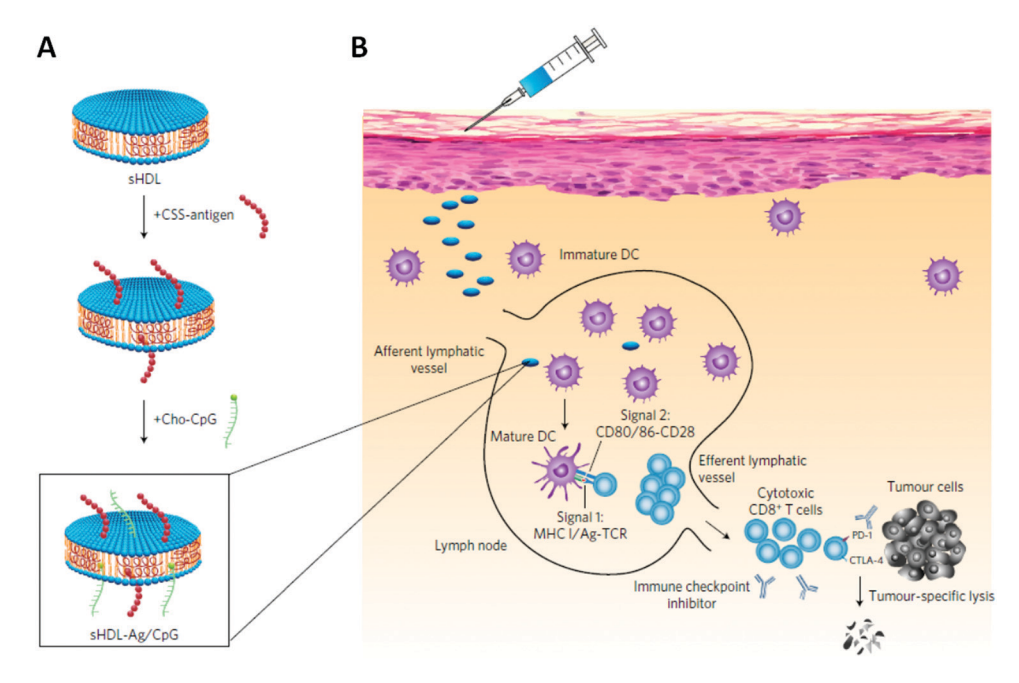


Fig. 9 NDs platform for personalized cancer vaccine delivery. (A) the NDs are composed of phospholipids and ApoA-1 mimetic peptides (22A) and post assembly loaded with cysteine-modified Ag peptides, including tumor-specific mutated neoantigens, and cholesterol-modified immunostimulatory molecules (Cho-CpG) (sHDL-Ag/CpG). (B) Following administration, NDs efficiently co-deliver Ag and CpG to draining lymph nodes, promote strong and durable Ag presentation by dendritic cells (DCs) (Signal 1), and induce DC maturation (Signal 2), eliciting a robust Ag-specific CD8C cytotoxic Tlymphocyte (CTL) responses. Activated CTLs recognize and kill their target cancer cells in peripheral tissues and exert strong anti-tumor efficacy. Combination immunotherapy with immune checkpoint blockade further amplifies the potency of ND vaccination, leading to elimination of established tumors. 126 Reproduced with the permission from ref. 126. Copyright 2017, Nature Publishing Group.

higher frequency of neoantigen-specific T cells compared with the intramuscular route, confirming the SC route as a more specific way to deliver a peptide vaccine to Delphian lymph nodes for immunotherapy against advanced cancers. 173

Cancer stem cells (CSCs) exist primarily in an inactive cell cycle and may escape from standard chemotherapy resulting in chemoresistance, tumor relapse, and metastasis. 174 Aldehyde dehydrogenase (ALDH) is a functional biomarker for CSCs and ALDH isoforms A1 and A3 are identified in human CSCs of melanoma and breast cancer patients. 175 Recently, Hassani Najafabadi et al. have identified antigenic sequences from ALDH1-A1 and ALDH1-A3 and used them to develop two antigenic peptides, LLYKLADLI from ALDH1-A1, and LLHQLADLV from ALDH1-A3. These antigenic peptides were loaded in LNDs constructed from apoA-1 mimetic peptides to activate APCs for T cell responses against ALDH CSCs. The LNDs loaded with cholesterol-CpG and antigen peptides form ALDH-A1-CpG-ND and ALDH-A3-CpG-ND and have particle diameters of 9-13 nm. The SC injection of NDs at the tail base of mice increased antigen trafficking to lymph nodes and generated robust ALDH-specific T cell responses in D5 melanoma and 4T1 cell mammary carcinoma mouse models. When NDs were combined with anti-PD-L1 (IgG), prolonged survival in both animal models indicates amplified immune response from the antigenic peptides and reduced the frequency of ALDH high CSCs in tumor tissues, leading to strong anti-tumor effects against both tumors. 176

In another example, Kuai et al. reported that NDs prepared with the apoA-1 mimetic peptide 22A loaded with 1,2-dioleoyl*sn-glycero-*3-phosphoethanolamine-*N-*[3-(2-pyridyldithio)] onate modified antigen E7 peptide (GQAEPDRAHYNIVTFCCKCD) and cholesterol-CpG induced a high E7 specific CD8+ T cell response (~32%). In TC-1 models of HPV-associated lung metastasis of head/neck and cervical cancer, the SC delivery of these NDs vaccines generated superior T cell responses resulting in the elimination of established TC-1 tumors. Another peptide, Gp33 (CSSKAVYNFATM), when loaded in NDs had a comparable T cell response and tumor regression rate with the Listeria-based live vector vaccine.31

Recently, Scheetz et al. developed three neoantigen peptides, namely AALLNKYLA (NeoAg1, H2-Db-restricted), MSLQFMTL (NeoAg2, H2-K<sup>b</sup>-restricted), and GAIFNGFTL (NeoAg3, H2-D<sup>b</sup>restricted) for immunotherapy and tested them in mice glioma models. All three neoantigen peptides and cholesterol-CpG can be loaded onto apoA-1 mimetic peptide-based sHDL and had a diameter of  $\sim$  12 nm. The cocktail NeoAgs-CpG-NDs vaccinationinduced robust expansion of IFNy leading to expression of neoantigen-specific CD8α<sup>+</sup> T cells. When the peptide ND treatment was combined with anti-PD-L1 (IgG) a robust induction in the maturation of intratumoral dendritic cells was observed, followed by intratumoral infiltration of  $CD8\alpha^{+}$  T cells and CD107α effector phenotype into the TME, leading to improved survival and protective immunity against tumor relapse. Importantly, the animals that survived from a combination treatment of NDs and the anti-PD-L1 group remained tumor-free without any treatment when rechallenged with GL261 cells. The sHDL loaded with peptide neoantigen epitopes (mIDH1123-132 and mIDH1<sub>126-141</sub>) in the genetically engineered murine mIDH1 glioma model significantly extended animal survival and provided long-term immunity against mIDH1 tumors. 177

### 4.5 Delivery of anticancer genes

Gene therapy is one of the effective therapeutic approaches for cancer treatment. <sup>178</sup> Cancer development initiates alteration of the oncogene, tumor suppressor gene, and other genes. Gene silencing reduces the expression of a specific gene in organisms being the promoter of tumor growth. RNA interference (RNAi) is the most commonly used technique for gene silencing. 179 The RNAi (e.g., small interfering RNA [siRNA]) effectively silent genes that are difficult to target with conventional approaches such as antibodies or small molecule inhibitors. 180 However, naked DNA or RNA are easily cleared by the phagocytes or nucleases and their cellular uptake is limited, and thus requires specific delivery vectors to reach cancer cells. 181 A variety of vectors such as non-viral lipids or protein carriers, including cholesterol, LIP, antibody protomer fusions, cyclodextrin NP, fusogenic peptides, aptamers, biodegradable polylactide copolymers, and polymers 182,183 had partial success with limitations such as toxicity, instability, and non-targeted delivery. Cationic NDs provide a suitable platform for gene delivery and can be used to load the genes on the corona. The electrostatic interaction of cationic NDs and anionic genes neutralizes the charge from the NDs and allows intracellular transportation. Another potential approach is to chemically modify the RNA with a lipophilic anchor to make it suitable for loading on the NDs.

One commonly activated gene in many tumors is the signal transducer and activator of transcription 3 (STAT3) that mediates key processes involved in malignant transformation and progression. 184 STAT3 silencing using small molecule inhibitors or non-specific delivery methods results in severe adverse effects. 185 The siRNA for STAT3 and focal adhesion kinase were loaded on rHDL by Shahzad et al. to treat ovarian and colorectal cancer, respectively. The rHDL is composed of apoA-1 and efficiently incorporates (>90%) of siRNA onto rHDL, which was pretreated with oligolysine peptides ( $\sim 40$ lysine residues) to neutralize the anionic charge for stabilization. The siRNA-loaded NDs had a diameter of  $\sim 10$  nm. The rHDL had a robust payload carrying capacity (up to 4 mg of siRNA/ml) with high stability and no siRNA leakage for up to 2 weeks. The STAT3 and focal adhesion kinase siRNA-loaded rHDLs produce a significant gene silencing and had a synergistic effect with DTX or oxaliplatin to reduce the tumor burden in both orthotopic mouse models. Combination treatment with STAT3 siRNA/rHDL and DTX had a 30-fold increase in tumor cell apoptosis in TME when compared with the control group, suggesting highly efficient delivery of siRNA to the target tissue. 180

In another study, Chen et al. developed STAT3 siRNA loaded on two different HNDs bearing cyclic RGD peptide (cRGD) to target  $\alpha_v \beta_3$  integrin receptors. The cRGD was attached to the HNDs either at the edge or to both planes to produce E-cRGD-NDs or P-cRGD-NDs, respectively (Fig. 4D). These HNDs had

high stability and rigid structure due to in situ polymerization of organosiloxane to form a sol-gel coating on the surface of the NDs. The empty HND has a particle diameter of  $\sim 50$  nm, whereas the siRNA loaded HNDs have a slightly larger size. The ligand anisotropy endowed the HNDs show diversified cellular interactions resulting in different efficacies for E-cRGD-NDs and P-cRGD-NDs. The edge modification of cRGD efficiently separated the targeting domain and siRNA loading field, thus establishing the functional anisotropy of NDs. This segregation resulted in the collaborative superiority in siRNA loading, cellular uptake, gene silencing efficiency, and protein expression when compared to P-cRGD-NDs and Lipofectamine 3000. This superiority of E-cRGD-NDs was further enhanced by co-administration of PTX, which showed the most significant tumor inhibition and resulted in almost complete tumor suppression, suggesting the potential benefits of anisotropic E-cRGD-NDs as a delivery platform for combined delivery of gene and chemotherapeutic agent. 127

In another example, Ghosh et al. reconstituted NDs using apoA-1 (particle diameter 20-50 nm) loaded with antisense siRNA for GAPDH after complexing dsOligo with the cationic lipid 1,2-dimyristoyl-3-trimethylammoniumpropane at a 1 to 1 charge ratio. The dsOligo complexed NDs induced ~60% knockdown of the GAPDH gene in HepG2 cells, a value comparable to that of Lipofectamine. 186

Besides these examples, some spherical HDL were also utilized as a vehicle for siRNA transport using surface-modified gold NP<sup>187</sup> or calcium phosphate 188 for siRNA loading in the HDL. In addition, conjugation of siRNA with cholesterol, bile acids, or long-chain fatty acids provides lipophilic siRNA that can be loaded in the rHDLs for high stability and higher cellular uptake. 189 The cholesterol-conjugated siRNA loaded in rHDLs were successfully utilized for Pokemon gene silencing in hepatocellular carcinoma. 190

# 5. HNDs for anticancer drug delivery

HNDs or hybrid bicelles (Fig. 2D) are a relatively new class of NDs. In contrast to conventional LNDs, HNDs are structurally stable and expect to retain their discoidal structure in long term in vivo, at elevated temperatures, or in the presence of other amphiphiles. The organic-inorganic hybrid bicelles are assembled using long-chain alkoxysilane lipids and short-chain phospholipids. Their high stability is achieved by the formation of a crosslinked siloxane network on the surface of HNDs via a sol-gel reaction of the organoalkoxysilane lipids. The resultant HNDs consist of a silicate surface encompassing a lipid bilayer, with typical diameters in the 20-50 nm range. HNDs are morphologically stable even after drying in the air or in the presence of an excessive nonionic surfactant. 90 The successful sol-gel reaction is often confirmed by Fourier-transformed infrared spectroscopy, which shows a peak at 1100 cm<sup>-1</sup> corresponding to the asymmetric stretching vibration of the siloxane bond (Si-O-Si), whereas morphology and size is confirmed by transmission cry-electron microscopy, small-angle X-ray scattering, dynamic light scattering and/or atomic force microscopy.

The HNDs can be easily modified with suitable ligands to target specific cancer receptors. Target specificity may be introduced by modifying either short alkyl chains that form the edges of HNDs (i.e., 1,2-dihexanoyl-sn-glycero-3-phosphochocholine (DHPC)) or long alkyl chains that form both planes of HNDs (i.e., CFL). For example, the octa arginine sequence of cell-penetrating peptides can be introduced to modify HNDs and enhance their penetration into cancer cells.<sup>27</sup> The lipid core of the HNDs is suitable for loading hydrophobic drugs such as DOX for cancer drug delivery.84,191 The partial silica coating on the HNDs improves their stability to a great extent while compromising the bilayer fluidity, which may retard drug release. However, drug release may be improved by doping lipid-modified PEG such as DSPE-PEG2000. Such modification improves drug release and enhances the therapeutic efficacy of the encapsulated drug.<sup>84</sup> Like targeting ligands, drugs may also be suitably modified to load into the lipid core or conjugate with short or long-chain lipid components.

In general, HNDs maintain their discoidal morphology above the phase transition temperature of long-chain lipids. 192 The siloxane bonds can be only degraded at very high temperatures 193 or at extreme chemical conditions (pH 2-4 and 9-12), 194 which present a challenge regarding their biodegradability. However, siloxane polymers are known for their low toxicity, good blood compatibility, and physiological inertness. 195 The uses of HNDs for the delivery of chemotherapeutics for cancer treatment have been explored in recent years.

Lin et al. fabricated HNDs from CFL and DHPC and loaded them with DOX, resulting in nanostructures with a diameter of  $\sim$  60 nm and a thickness of  $\sim$  6 nm. These HNDs had a DOX loading efficiency of  $\sim 2\%$  without affecting particle size and showed extended stability on long-term storage or in the presence of nonionic detergent. The HNDs displayed high cellular uptake via endocytosis related to clathrin and micropinocytosis and showed pH-dependent DOX release. The pH sensitivity is most likely due to the protonation of the DHPC at low pH and subsequent disruption of the nanostructure. 191

The silica coating on the lipid NDs may retard the encapsulated drug release, whereas incorporating a permeability enhancer in the lipid bilayer may increase membrane fluidity and enhance drug release. To study such an effect, Lin et al. assembled HNDs with different concentrations of PEG dopped in the lipid bilayer and monitored DOX release. Among various combinations, HNDs prepared by 5% PEG doping proved best and had high DOX loading of ~2.4% (DOX@HNDs) with a particle diameter of  $\sim 50$  nm and discoidal morphology. The DOX in HNDs exhibited higher cellular uptake and therapeutic efficacies than free DOX in mice model.84

Along with the shape of NPs, target biological cells have a crucial impact on cellular behavior for the bio-nano interactions. The effect of shape anisotropy, functionalization anisotropy, and phagocytic/endocytic nature of cells was screened by Wang et al., who compared hybrid nanospheres, HNDs, as well as HNDs with edge modification and plane modification. The HNDs prepared from CFL and a DHPC were decorated with the octaarginine sequence of cell-penetrating peptides after

conjugating with short alkyl chain (C8-R8) and long alkyl chain (C18-R8), respectively, for edge or plane modification. The HNDs had a diameter of  $\sim 50$  nm and a thickness of  $\sim 5$  nm. The shape anisotropy significantly influenced the cellular internalization and followed a regular rule: strong phagocytic cells were more sensitive to the change in ligand location but relatively insensitive to the alteration in shape, whereas the weak-phagocytic cells were the opposite. The shape anisotropy effect is most likely because plane modified HNDs might firmly adhere to the cell surface via its larger contact area and up to 50% of active R8, which impeded the biomembrane motion, resulting in decreased membrane fluidity. In contrast, edgemodified HNDs might contact the cell membrane on its R8 modified edge, and such a small contact area might lead to less restriction to the cell membrane fluidity.<sup>27</sup>

**Review Article** 

# 6. PNDs as a versatile new ND platform for cancer therapy

The most recently discovered PNDs are potentially another powerful ND platform for cancer diagnostic and treatment (Fig. 2C). PNDs support membrane proteins as LNDs but with much improved stability. Unlike LNDs that tend to aggregate in 1–2 days even when stored at 4  $^{\circ}$ C and in a few hours at elevated temperatures, PNDs are largely stable at 4 °C, room temperature, or 37 °C for at least one week that was tested. 36 PNDs differ from LNDs in that the lipid bilayer of LNDs is replaced by

a patch of amphiphilic block copolymer membrane, which in turn is encased and stabilized by the same choices of membrane scaffold macromolecules as used in LNDs.36 Those amphiphilic block copolymers by themselves self-assemble in aqueous solution into polymersomes, the synthetic analogues of lipid vesicles. 196,197 The amphiphilic block copolymers (di-block, AB; or triblock, ABA or ABC type polymers) contain adjacent blocks with different compositions, solubility, and sequence distributions. Depending on the hydrophobic block sizes, polymersomes can be several folds thicker compared to LIP, enabling mechanical and chemical stability and decreasing the premature release of encapsulated payloads. 198 Polymersomes offer benefits due to the customizable and flexible design of copolymers, enabling improved control over properties such as size, surface charge, functionalization, and architecture, along with increased complexity in design, such as stimuli responsiveness. 199,200

The polymersome-forming characteristic of amphiphilic block copolymers is the prerequisite for their self-assembly with membrane scaffold macromolecules into PNDs. The morphology of self-assembled amphiphilic block polymers depends on the packing of copolymer chains, which can be determined based on the 'packing parameter' p. 201 In practice though, it is difficult to calculate p based on the structure of the amphiphilic block polymers. Alternatively, block copolymers can be characterized by a synthetically accessible hydrophilic block fraction  $(f_{\text{hydrophilic}})$ . As a simple rule of thumb, a  $f_{\text{hydrophilic}}$  of approximately 35  $\pm$  10% of an amphiphilic diblock copolymer yields

Table 2 Examples of polymersome-forming amphiphilic block polymers used for cancer drug delivery

No.	Polymer	Hydrophilic block	Hydrophobic block	Molecular wt (kD)	$f_{ m hydrophilic}$	Ref.
Diblo	ck polymers, AB					
1	PEO <sub>40</sub> -PEE <sub>37</sub>	PEO	PEE	3.9	0.39	204
2	$PEO_{26}-PBD_{46}$	PEO	PBD	3.6	0.28	204
3	PEG <sub>45</sub> -PBOx <sub>48</sub>	PEG	PBOx	10	_	205
4	$PIAT_{50}-PS_{40}$	PIAT	PS	_	_	206
5	$PEO_{46}$ - $PCL_{24}$	PEO	PCL	4.7	0.42	207
6	$PEO_{43}$ - $PLA_{44}$	PEO	PLA	6	0.33	207
7	$PEO_{80}-PBD_{125}$	PEO	PBD	10.4	0.29	207
8	PEG <sub>45</sub> -PCL <sub>29</sub> ; DEX <sub>22</sub> -PCL <sub>66</sub>	PEG; DEX	PCL	DEX-PCL = 17.8;	DEX-PCL = 0.32;	208
				PEG-PCL = 5.3	PEG-PCL = 0.37	
9	PEG <sub>114</sub> -PLGA <sub>38</sub>	PEG	PLGA	10	_	209
10	PAA <sub>16</sub> -ONB-PMCL <sub>76</sub>	PAA	PMCL	11.3	0.11	210
11	$PTMC_{26}$ - $b$ - $PGA_{20}$	PGA	PTMC	5.2	_	211
12	$PEG_{114}-P(TMC_{190}-DTC_{29})$	PEG	P(TMC-co-DTC)	24.2	_	212
13	PEG <sub>17</sub> -PPS <sub>30</sub>	PEG	PSS	2.7	0.28	213
14	$PMPC_{25}-PDPA_{120}$	PMPC	PDPA	55.0	_	214
15	$PEO_{43}-P(DEA_{94}-CMA_{5})$	PEO	P(DEA-CMA)	17.7	_	215
16	PGMA <sub>58</sub> -PHPMA <sub>250</sub>	PGMA	PHPMA	58.9	_	216
17	$PEO_{45}$ -PTTAMA <sub>25</sub>	PEO	PTTAMA	13.6	_	217
18	PEG45-P(Asp)100; PEG45-P(Asp-AE)100	PEG	PAsp; P(Asp-AE)	_	_	218
Trible	ock polymers, ABA and ABC					
1	PMOXA <sub>25</sub> -PDMS <sub>75</sub> -PMOXA <sub>25</sub>	PMOXA	PDMS	9.8	_	219
2	PLA <sub>115</sub> -F127-PLA <sub>115</sub>	F127	PLA	29	_	220
3	$PEO_{45}$ - $PLA_{85}$ - $PAA_{110}$	PEO and PAA	PLA	19.5	_	221
4	$PEG_{114}$ - $PCL_{160}$ - $PDEA_{24}$	PEG and PDEA	PCL	27.3	_	222
5	$P(EO_{196}$ - $co$ - $AGE_9)$ - $g$ - $PCL_{237}$	P(EO-co-AGE)	PCL	13.8	0.27	223
6	$PEG_{114}$ - $P(CL$ - $co$ - $LA)_{59}$ - $PEG_{45}$	PEG	CL-co-LA	50.5	0.38	224
7	$P(LA_{123}$ - $co$ - $DAC_{3.5})$ - $g$ - $PEG_{114}$	PEG	P(LA-co-DAC)	15	0.33	225
8	$PEG_{113}$ -PAA <sub>20</sub> -PNIPAM <sub>211</sub>	PEG and PAA	PNIPAM	26.44	_	226

polymersomes; 202,203 Other nanostructure morphologies such as micelles and worm-like micelles are obtained at  $f_{\text{hydrophilic}}$  > 0.50, while inverse micelles or solid-like particles are observed at  $f_{\text{hydrophilic}} < 0.20.^{198}$  This simple rule may not apply to amphiphilic triblock copolymers though. An incomplete list of reported amphiphilic blocks polymers used to construct polymersomes for cancer drug delivery is presented in Table 2. All of those block copolymers are potential candidates for the assembly of PNDs.

Like LNDs and HNDs, PNDs can be modified for drug delivery to cancer cells by similar synthetic strategies. PNDs offer distinct advantages over LNDs and HNDs, such as improved stability, facile conjugation chemistry, and biodegradability. PNDs may be fine-tuned by carefully selecting polymer blocks with desired functionality for degradation in stimuli-responsive manners such as elevated pH, TME redox potential, or sensitivity to specific enzymes, as that explored in the design of polymersome-based drug delivery systems. 227-230 Similarly, the thermal stability and biodegradability of the PNDs may also be tailor-made through permutation and combination from a large array of synthetic block polymers. 231-234 PNDs may accommodate lipophilic drugs in the hydrophobic core or conjugated to the copolymer backbone through chemoresponsive linkages. The mechanism of chemo-responsiveness and drug release relies on the disassembly or swelling of nanocarriers in response to the actions of organic molecules or enzymes in the TME. 235-237 This phenomenon can be applied to PNDs for controlled delivery of drugs triggered by a disease-related abnormal level of chemicals in the TME, such as acidic pH, hypoxic microenvironment, elevated levels of reactive oxygen species, and essential enzymes (i.e. MMP-9, MMP-2, cathepsin B, FAP-α, legumain, etc.). 237,238

### 7. Future directions and outlook

The lipid-based NDs including LNDs and SMALPs showed continuous aggregation during storage even at low temperature, which jeopardizes the reliability and efficacy of ND-based drug formulations. The clinical translation of MSP or apoA-1 mimetic peptides based NDs is also partially limited by the high production cost of large quantities of pure apoA-1 proteins either recombinantly or by plasma-purification. 148 In addition, the use of MSP and apoA-1 to encase NDs raises potential safety concerns due to their human protein origin,239 and post-translational modifications of apoA-1 that occur in the context of systemic inflammation (oxidative damage, glycation or cabamylation) may transform anti-inflammatory apoA-1 into a pro-inflammatory protein. Humoral autoimmunity to apoA-1 and HDL indicative of modulated inflammatory and immune responses was indeed observed in populations of high cardiovascular risk.<sup>240</sup>

Significant developments in the constitutional elements of NDs have taken place in recent years, expanding the horizon to exploit NDs for cancer mitigation. For example, to circumvent the often fluidic and labile nature of LNDs, HNDs were developed and showed remarkable stability even at elevated

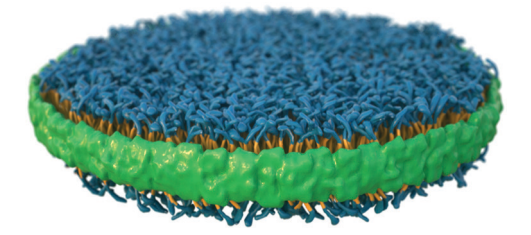


Fig. 10 Proposed structure of fully synthetic PNDs. A nanoscale membrane patch comprised of amphiphilic block copolymers (blue: hydrophilic block; gold: hydrophobic block) is encased and stabilized by amphipathic belt-like polymers (green).

temperatures and/or under drying conditions. On the downside, the larger particle sizes of HNDs, their limited choices of constitutional components, difficult body clearance, and potential organ accumulation may limit their clinical applications. Another very promising development for anticancer drug delivery is PNDs, i.e., the lipid bilayer of the NDs is replaced with an amphiphilic block copolymer membrane in the formation of MSP-encased PNDs.36 We expect that the MSPs derived from apoA-1, the essential constitutional element of the NDs, may be also replaced with fully synthetic small peptides<sup>111,123,126,148,168</sup> or synthetic amphipathic random copolymers such as SMAs<sup>33-37</sup> and many of the SMA-like alternatives. 85,241 The enhanced buffer stability of zwitterionic SMAs and other SMA-like copolymers in the presence of divalent cations or under low pH environment expands their utility to support NDs for pharmaceutical applications. 35,85,86,241,242 With the exciting potential of NDs for cancer therapy as well as some of their outstanding challenges in mind, we envision that the flexibility of the self-assembly process that produces NDs may open up a new avenue to realize fully synthetic PNDs (Fig. 10).

The fully synthetic PNDs will consist of suitable amphiphilic block copolymers that form the hydrophobic membrane patch, and amphiphilic SMA-like random copolymers that act as the membrane scaffold to encase and stabilize the NDs. By taking advantage of the expertise gained during the last two decades on the molecular engineering of polymer-based drug delivery systems,243-247 this new type of fully synthetic PNDs can be designed to have the long shelf life needed for industry-scale drug formulations, and the versatility to deliver a wide range of anti-cancer agents to tumor sites with high specificity, efficiency, serum stability, low toxicity, and excellent biodegradability.

## 8. Conclusion

The clinical translation of nanomedicines is challenging due to various limiting factors such as controlled and reproducible synthesis at the industrial scale, stability of drug formulations before and after drug administration, inconsistent toxicity, and differences in efficacy between benchtop tests and clinical trials, just to name a few. Many of the challenges come from poorly understood in vivo responses to nanomedicines. For example, NPs properties such as size, shape, and targeting ligands can be

Review Article Chem Soc Rev

significantly altered from the original designs once in the bloodstream. The interaction of nanomedicines with plasma proteins in the bloodstream forms a 'corona' around the NPs that redefines their pharmacokinetics and targeting efficiency. Although second-generation nanomedicines are actively pursued for cancer diagnostic and treatment, many of the conventional spherical NP-based formulations proved inefficient in clinical trials. For example, it has been found that the complex biological barriers result in suboptimal therapeutic benefits, as <1% (median) of the NPs generally reach the tumor sites.  $^{248}$ 

NDs, including LNDs, PNDs, and HNDs, have immerged as effective tools for delivering diagnostic and chemotherapeutic agents to cancer cells. We discussed many examples where NDs effectively delivered diagnostic agents, including agents for fluorescent imaging, MRI, CT, and PET, along with chemotherapeutic agents, peptide-based cancer vaccines, and therapeutic genes (siRNA). Notably, cellular internalization of NDs is not limited to the EPR effect since they are taken up following the binding to their natural receptors (SR-B1) or receptors of choice by adding specific receptor–ligand on the NDs. This is an important property of NDs, as it was shown recently that the EPR effect by itself is not sufficient to account for the observed number of NPs in a cancer cell.<sup>249</sup>

Looking forward, we believe that the field of adapting NDs for drug delivery in general and cancer mitigation in particular, has great potential to grow. Developing fully synthetic PNDs as nanocarriers for the diagnosis and treatment of cancers is a new frontier waiting to be explored.

## **Abbreviations**

co-LA)-PEG

PEO-PEE	poly(ethyleneoxide)-poly(ethylethylene)			
PEO-PBD	poly(ethyleneoxide)-poly(butadiene)			
PBOx	poly(styreneboroxole)			
PEG	poly(ethylene glycol)			
PMOXA-PDMS-				
PMOXA	poly[(2-methyloxazoline)-poly(dimethyl-			
	siloxane)-poly(2-methyloxazoline)]			
PS-PIAT	poly[styrene-b-poly(1-isocyanoalanine(2-			
	thiophen-3-yl-ethyl) amide)]			
PLA-F127-PLA	poly(lactic acid)- <i>b</i> -Pluronic F127- <i>b</i> -			
	poly(lactic acid)			
PEO-b-PCL-b-PAA	poly(ethylene oxide)-b-poly(caprolactone)-			
	b-poly(acrylic acid)			
PEO-b-PCL	poly(ethylene oxide)- <i>b</i> -poly(ε-caprolactone)			
PEG-PCL-PDEA	poly(ethylene glycol)-b-poly(e-caprolactone)-			
	<i>b</i> -poly(2-(diethylamino) ethyl methacrylate)			
DEX-PCL	dextran- $b$ -poly( $\epsilon$ -caprolactone)			
PEAG	poly(ethylene oxide-co-allyl glycidyl ether)			
PEG-b-PLGA	poly(ethylene glycol)- <i>b</i> -poly(L-lactic- <i>co</i> -			
	glycolic acid)			
mPEG-P(CL-	<del>57)</del>			

methylated poly(ethylene glycol)-b-poly-

(caprolactone-co-lactide)-b-poly(ethylene

P(LA-co-DAC)-g-PEG poly(lactide-co-diazidomethyl trimethylene carbonate)-g-poly(ethylene glycol) PAA-ONB-PMCL poly(acrylic acid)-ONB-poly(methyl caprolactone) PTMC-b-PGA poly(trimethylene carbonate)-b-poly(Lglutamic acid) PEG-P(TMC-DTC) poly(ethylene glycol)-b-poly(trimethylene carbonate-co-dithiolane trimethylene carbonate) PEG-PPS poly(ethylene glycol)-b-poly(propylene sulfide) PMPC-PDPA poly(2-(methacryloyloxy)ethyl phosphorylcholine)-b-poly(2-(diisopropylamino)ethyl methacrylate) PGMA-PHPMA poly(glycerol monomethacrylate)-b-poly(2hydroxypropyl methacrylate) PEO-b-PTTAMA poly(ethylene oxide)-b-poly(2-(((5-methyl-2-(2,4,6-trimethoxyphenyl)-1,3-dioxan-5-yl)methoxy)carbonyl)amino)ethyl methacrylate) PEG-P(Asp) poly(ethylene glycol)-b-poly(aspartic acid) glycol)-b-poly([2-amino-PEG-P(Asp-AE) poly(ethylene ethyl]-aspartamide) PEG-PAA-PNIPAM poly(ethylene oxide)-b-poly(acrylic acid)-b-

## Author contributions

The manuscript is written through contributions from all authors. All authors approved the final manuscript.

poly(N-isopropylacrylamide)

### Conflicts of interest

The authors declare no competing interests.

# Acknowledgements

This work was supported in part by the Cancer Prevention and Research Institute of Texas (CPRIT) (RP180827), the National Science Foundation (NSF DMR-1810767), the South Plains Foundation, and the <u>CH</u> Foundation. Fig. 1 and 3 were created with BioRender.com.

### References

- 1 Y. Peng, J. Bariwal, V. Kumar, C. Tan and R. I. Mahato, Organic Nanocarriers for Delivery and Targeting of Therapeutic Agents for Cancer Treatment, *Adv. Ther.*, 2020, 3, 1900136.
- 2 P. Guo, J. Huang and M. A. Moses, Cancer Nanomedicines in an Evolving Oncology Landscape, *Trends Pharmacol. Sci.*, 2020, **41**, 730–742.
- 3 K. O. Alfarouk, C. M. Stock, S. Taylor, M. Walsh, A. K. Muddathir, D. Verduzco, A. H. Bashir, O. Y. Mohammed, G. O. Elhassan, S. Harguindey, S. J. Reshkin, M. E. Ibrahim

glycol)

- and C. Rauch, Resistance to cancer chemotherapy: failure in drug response from ADME to P-gp, *Cancer Cell Int.*, 2015, **15**, 71.
- 4 W. Mu, Q. Chu, Y. Liu and N. Zhang, A Review on Nano-Based Drug Delivery System for Cancer Chemoimmunotherapy, *Nano-Micro Lett.*, 2020, **12**, 142.
- 5 Y. Wang and D. S. Kohane, External triggering and triggered targeting strategies for drug delivery, *Nat. Rev. Mater.*, 2017, 2, 17020.
- 6 T. Sun, A. Dasgupta, Z. Zhao, M. Nurunnabi and S. Mitragotri, Physical triggering strategies for drug delivery, Adv. Drug Delivery Rev., 2020, 158, 36–62.
- 7 J. Shi, P. W. Kantoff, R. Wooster and O. C. Farokhzad, Cancer nanomedicine: progress, challenges and opportunities, *Nat. Rev. Cancer*, 2017, 17, 20–37.
- 8 D. F. Costa and V. P. Torchilin, Micelle-like nanoparticles as siRNA and miRNA carriers for cancer therapy, *Biomed. Microdevices*, 2018, 20, 59.
- 9 G. Cavallaro, C. Sardo, E. F. Craparo, B. Porsio and G. Giammona, Polymeric nanoparticles for siRNA delivery: Production and applications, *Int. J. Pharm.*, 2017, 525, 313–333.
- 10 A. Sharma, N. K. Jha, K. Dahiya, V. K. Singh, K. Chaurasiya, A. N. Jha, S. K. Jha, P. C. Mishra, S. Dholpuria, R. Astya, P. Nand, A. Kumar, J. Ruokolainen and K. K. Kesari, Nanoparticulate RNA delivery systems in cancer, *Cancer Rep.*, 2020, 3, e1271.
- 11 H. J. Kim, A. Kim, K. Miyata and K. Kataoka, Recent progress in development of siRNA delivery vehicles for cancer therapy, *Adv. Drug Delivery Rev.*, 2016, **104**, 61–77.
- 12 M. J. Mitchell, M. M. Billingsley, R. M. Haley, M. E. Wechsler, N. A. Peppas and R. Langer, Engineering precision nanoparticles for drug delivery, *Nat. Rev. Drug Discovery*, 2021, 20, 101–124.
- 13 A. Aghebati-Maleki, S. Dolati, M. Ahmadi, A. Baghbanzhadeh, M. Asadi, A. Fotouhi, M. Yousefi and L. Aghebati-Maleki, Nanoparticles and cancer therapy: Perspectives for application of nanoparticles in the treatment of cancers, *J. Cell Physiol.*, 2020, 235, 1962–1972.
- 14 J. Wolfram and M. Ferrari, Clinical Cancer Nanomedicine, *Nano Today*, 2019, 25, 85–98.
- 15 H. He, L. Liu, E. E. Morin, M. Liu and A. Schwendeman, Survey of Clinical Translation of Cancer Nanomedicines-Lessons Learned from Successes and Failures, *Acc. Chem. Res.*, 2019, **52**, 2445–2461.
- 16 W. Yang, H. Veroniaina, X. Qi, P. Chen, F. Li and P. C. Ke, Soft and Condensed Nanoparticles and Nanoformulations for Cancer Drug Delivery and Repurpose, *Adv. Ther.*, 2020, 3, 1900102.
- 17 D. Hwang, J. D. Ramsey and A. V. Kabanov, Polymeric micelles for the delivery of poorly soluble drugs: From nanoformulation to clinical approval, *Adv. Drug Delivery Rev.*, 2020, **156**, 80–118.
- 18 F. Soetaert, P. Korangath, D. Serantes, S. Fiering and R. Ivkov, Cancer therapy with iron oxide nanoparticles: Agents of thermal and immune therapies, *Adv. Drug Delivery Rev.*, 2020, **163–164**, 65–83.

- 19 D. Bobo, K. J. Robinson, J. Islam, K. J. Thurecht and S. R. Corrie, Nanoparticle-Based Medicines: A Review of FDA-Approved Materials and Clinical Trials to Date, *Pharm. Res.*, 2016, 33, 2373–2387.
- 20 A. C. Anselmo and S. Mitragotri, Nanoparticles in the clinic: An update, *Bioeng. Transl. Med.*, 2019, 4, e10143.
- 21 S. Raj, S. Khurana, R. Choudhari, K. K. Kesari, M. A. Kamal, N. Garg, J. Ruokolainen, B. C. Das and D. Kumar, Specific targeting cancer cells with nanoparticles and drug delivery in cancer therapy, *Semin. Cancer Biol.*, 2021, 69, 166–177.
- 22 O. Borgå, R. Henriksson, H. Bjermo, E. Lilienberg, N. Heldring and N. Loman, Maximum Tolerated Dose and Pharmacokinetics of Paclitaxel Micellar in Patients with Recurrent Malignant Solid Tumours: A Dose-Escalation Study, Adv. Ther., 2019, 36, 1150–1163.
- 23 R. Kuai, D. Li, Y. E. Chen, J. J. Moon and A. Schwendeman, High-Density Lipoproteins: Nature's Multifunctional Nanoparticles, ACS Nano, 2016, 10, 3015–3041.
- 24 B. A. Kingwell, M. J. Chapman, A. Kontush and N. E. Miller, HDL-targeted therapies: progress, failures and future, *Nat. Rev. Drug Discovery*, 2014, 13, 445–464.
- 25 K. C. Vickers, B. T. Palmisano, B. M. Shoucri, R. D. Shamburek and A. T. Remaley, MicroRNAs are transported in plasma and delivered to recipient cells by high-density lipoproteins, *Nat. Cell Biol.*, 2011, 13, 423–433.
- 26 A. Chen, E. J. Majdinasab, M. C. Fiori, H. J. Liang and G. A. Altenberg, Polymer-Encased Nanodiscs and Polymer Nanodiscs: New Platforms for Membrane Protein Research and Applications, *Front. Bioeng. Biotechnol.*, 2020, 8, 598450.
- 27 X. Wang, L. Lin, R. Liu, M. Chen, B. Chen, B. He, B. He, X. Liang, W. Dai, H. Zhang, X. Wang, Y. Wang, Z. Dai and Q. Zhang, Anisotropy in Shape and Ligand-Conjugation of Hybrid Nanoparticulates Manipulates the Mode of Bio-Nano Interaction and Its Outcome, *Adv. Funct. Mater.*, 2017, 27, 1700406.
- 28 T. H. Bayburt, Y. V. Grinkova and S. G. Sligar, Self-Assembly of Discoidal Phospholipid Bilayer Nanoparticles with Membrane Scaffold Proteins, *Nano Lett.*, 2002, 2, 853–856.
- 29 I. G. Denisov and S. G. Sligari, Nanodiscs in Membrane Biochemistry and Biophysics, *Chem. Rev.*, 2017, 117, 4669–4713.
- 30 K. Popovic, J. Holyoake, R. Pomes and G. G. Prive, Structure of saposin A lipoprotein discs, *Proc. Natl. Acad. Sci. U. S. A.*, 2012, **109**, 2908–2912.
- 31 R. Kuai, P. B. Singh, X. Sun, C. Xu, A. Hassani Najafabadi, L. Scheetz, W. Yuan, Y. Xu, H. Hong, D. B. Keskin, C. J. Wu, R. Jain, A. Schwendeman and J. J. Moon, Robust Anti-Tumor T Cell Response with Efficient Intratumoral Infiltration by Nanodisc Cancer Immunotherapy, *Adv. Ther.*, 2020, 3, 2000094.
- 32 K. Iric, M. Subramanian, J. Oertel, N. P. Agarwal, M. Matthies, X. Periole, T. P. Sakmar, T. Huber, K. Fahmy and T. L. Schmidt, DNA-encircled lipid bilayers, *Nanoscale*, 2018, 10, 18463–18467.

Review Article Chem Soc Rev

- 33 T. J. Knowles, R. Finka, C. Smith, Y. P. Lin, T. Dafforn and M. Overduin, Membrane proteins solubilized intact in lipid containing nanoparticles bounded by styrene maleic acid copolymer, *J. Am. Chem. Soc.*, 2009, **131**, 7484–7485.
- 34 J. M. Dorr, S. Scheidelaar, M. C. Koorengevel, J. J. Dominguez, M. Schafer, C. A. van Walree and J. A. Killian, The styrene-maleic acid copolymer: a versatile tool in membrane research, *Eur. Biophys. J.*, 2016, **45**, 3–21.
- 35 M. C. Fiori, Y. Jiang, G. A. Altenberg and H. Liang, Polymerencased nanodiscs with improved buffer compatibility, *Sci. Rep.*, 2017, 7, 7432.
- 36 M. C. Fiori, Y. Jiang, W. Zheng, M. Anzaldua, M. J. Borgnia, G. A. Altenberg and H. Liang, Polymer Nanodiscs: Discoidal Amphiphilic Block Copolymer Membranes as a New Platform for Membrane Proteins, *Sci. Rep.*, 2017, 7, 15227.
- 37 A. Chen, E. J. Majdinasab, M. C. Fiori, H. Liang and G. A. Altenberg, Polymer-Encased Nanodiscs and Polymer Nanodiscs: New Platforms for Membrane Protein Research and Applications, *Front. Bioeng. Biotechnol.*, 2020, 8, 598450.
- 38 S. Senapati, A. K. Mahanta, S. Kumar and P. Maiti, Controlled drug delivery vehicles for cancer treatment and their performance, *Signal Transduction Targeted Ther.*, 2018, 3, 7.
- 39 P. N. Navya, A. Kaphle, S. P. Srinivas, S. K. Bhargava, V. M. Rotello and H. K. Daima, Current trends and challenges in cancer management and therapy using designer nanomaterials, *Nano Convergence*, 2019, 6, 23.
- 40 R. van der Meel, E. Sulheim, Y. Shi, F. Kiessling, W. J. M. Mulder and T. Lammers, Smart cancer nanomedicine, *Nat. Nanotechnol.*, 2019, 14, 1007–1017.
- 41 L. Zhou, P. Zhang, H. Wang, D. Wang and Y. Li, Smart Nanosized Drug Delivery Systems Inducing Immunogenic Cell Death for Combination with Cancer Immunotherapy, Acc. Chem. Res., 2020, 53, 1761–1772.
- 42 J. Nam, S. Son, K. S. Park, W. Zou, L. D. Shea and J. J. Moon, Cancer nanomedicine for combination cancer immunotherapy, *Nat. Rev. Mater.*, 2019, 4, 398–414.
- 43 K. A. Afonin, M. A. Dobrovolskaia, G. Church and M. Bathe, Opportunities, Barriers, and a Strategy for Overcoming Translational Challenges to Therapeutic Nucleic Acid Nanotechnology, ACS Nano, 2020, 14, 9221–9227.
- 44 W. Yan, S. S. Leung and K. K. To, Updates on the use of liposomes for active tumor targeting in cancer therapy, *Nanomedicine*, 2020, **15**, 303–318.
- 45 E. Beltrán-Gracia, A. López-Camacho, I. Higuera-Ciapara, J. B. Velázquez-Fernández and A. A. Vallejo-Cardona, Nanomedicine review: clinical developments in liposomal applications, *Cancer Nanotechnol.*, 2019, 10, 11.
- 46 B. Ghosh and S. Biswas, Polymeric micelles in cancer therapy: State of the art, *J. Controlled Release*, 2021, 332, 127–147.
- 47 Z. Wan, R. Zheng, P. Moharil, Y. Liu, J. Chen, R. Sun, X. Song and Q. Ao, Polymeric Micelles in Cancer Immunotherapy, *Molecules*, 2021, 26, 1220.
- 48 S. Busatto, S. A. Walker, W. Grayson, A. Pham, M. Tian, N. Nesto, J. Barklund and J. Wolfram, Lipoprotein-based drug delivery, Adv. Drug Delivery Rev., 2020, 159, 377–390.

- 49 K. M. Wasan, D. R. Brocks, S. D. Lee, K. Sachs-Barrable and S. J. Thornton, Impact of lipoproteins on the biological activity and disposition of hydrophobic drugs: implications for drug discovery, *Nat. Rev. Drug Discovery*, 2008, 7, 84–99
- 50 R. O. Ryan, Nanodisks: hydrophobic drug delivery vehicles, *Expert Opin. Drug Delivery*, 2008, **5**, 343–351.
- 51 S. T. Chuang, S. Cruz and V. Narayanaswami, Reconfiguring Nature's Cholesterol Accepting Lipoproteins as Nanoparticle Platforms for Transport and Delivery of Therapeutic and Imaging Agents, *Nanomaterials*, 2020, 10, 906.
- 52 K. M. McMahon and C. S. Thaxton, High-density lipoproteins for the systemic delivery of short interfering RNA, *Expert Opin. Drug Delivery*, 2014, 11, 231–247.
- 53 W. J. M. Mulder, M. M. T. van Leent, M. Lameijer, E. A. Fisher, Z. A. Fayad and C. Pérez-Medina, High-Density Lipoprotein Nanobiologics for Precision Medicine, Acc. Chem. Res., 2018, 51, 127–137.
- 54 I. G. Denisov and S. G. Sligar, Nanodiscs in Membrane Biochemistry and Biophysics, *Chem. Rev.*, 2017, **117**, 4669–4713.
- 55 S. G. Sligar and I. G. Denisov, Nanodiscs: A toolkit for membrane protein science, *Protein Sci.*, 2021, 30, 297–315.
- 56 M. Esmaili, M. A. Eldeeb and A. A. Moosavi-Movahedi, Current Developments in Native Nanometric Discoidal Membrane Bilayer Formed by Amphipathic Polymers, *Nanomaterials*, 2021, 11.
- 57 M. D. Farrelly, L. L. Martin and S. H. Thang, Polymer Nanodiscs and Their Bioanalytical Potential, *Chemistry*, 2021, 27, 12922–12939.
- 58 A. B. Jindal, The effect of particle shape on cellular interaction and drug delivery applications of micro- and nanoparticles, *Int. J. Pharm.*, 2017, 532, 450–465.
- 59 R. Toy, P. M. Peiris, K. B. Ghaghada and E. Karathanasis, Shaping cancer nanomedicine: the effect of particle shape on the in vivo journey of nanoparticles, *Nanomedicine*, 2014, 9, 121–134.
- 60 X. Xie, J. Liao, X. Shao, Q. Li and Y. Lin, The Effect of shape on Cellular Uptake of Gold Nanoparticles in the forms of Stars, Rods, and Triangles, *Sci. Rep.*, 2017, 7, 3827.
- 61 M. C. Arno, M. Inam, A. C. Weems, Z. Li, A. L. A. Binch, C. I. Platt, S. M. Richardson, J. A. Hoyland, A. P. Dove and R. K. O'Reilly, Exploiting the role of nanoparticle shape in enhancing hydrogel adhesive and mechanical properties, *Nat. Commun.*, 2020, 11, 1420.
- 62 A. Banerjee, J. Qi, R. Gogoi, J. Wong and S. Mitragotri, Role of nanoparticle size, shape and surface chemistry in oral drug delivery, *J. Controlled Release*, 2016, 238, 176–185.
- 63 X. Huang, X. Teng, D. Chen, F. Tang and J. He, The effect of the shape of mesoporous silica nanoparticles on cellular uptake and cell function, *Biomaterials*, 2010, **31**, 438–448.
- 64 S. Y. Lee, M. Ferrari and P. Decuzzi, Shaping nano-/microparticles for enhanced vascular interaction in laminar flows, *Nanotechnology*, 2009, 20, 495101.
- 65 F. Gentile, C. Chiappini, D. Fine, R. C. Bhavane, M. S. Peluccio, M. M. Cheng, X. Liu, M. Ferrari and

- P. Decuzzi, The effect of shape on the margination dynamics of non-neutrally buoyant particles in twodimensional shear flows, J. Biomech., 2008, 41, 2312-2318.
- 66 G. Adriani, M. D. de Tullio, M. Ferrari, F. Hussain, G. Pascazio, X. Liu and P. Decuzzi, The preferential targeting of the diseased microvasculature by disk-like particles, Biomaterials, 2012, 33, 5504-5513.
- 67 H. T. Ta, N. P. Truong, A. K. Whittaker, T. P. Davis and K. Peter, The effects of particle size, shape, density and flow characteristics on particle margination to vascular walls in cardiovascular diseases, Expert Opin. Drug Delivery, 2018, 15, 33-45, DOI: 10.1080/17425247.2017.1316262.
- 68 P. A. Netti, S. Roberge, Y. Boucher, L. T. Baxter and R. K. Jain, Effect of transvascular fluid exchange on pressureflow relationship in tumors: a proposed mechanism for tumor blood flow heterogeneity, Microvasc. Res., 1996, 52, 27-46.
- 69 W. A. Hild, M. Breunig and A. Goepferich, Quantum dots nano-sized probes for the exploration of cellular and intracellular targeting, Eur. J. Pharm. Biopharm., 2008, 68, 153-168.
- 70 K. Zhang, H. Fang, Z. Chen, J. S. Taylor and K. L. Wooley, Shape effects of nanoparticles conjugated with cellpenetrating peptides (HIV Tat PTD) on CHO cell uptake, Bioconjugate Chem., 2008, 19, 1880-1887.
- 71 R. Agarwal, V. Singh, P. Jurney, L. Shi, S. V. Sreenivasan and K. Roy, Mammalian cells preferentially internalize hydrogel nanodiscs over nanorods and use shape-specific uptake mechanisms, Proc. Natl. Acad. Sci. U. S. A., 2013, 110, 17247-17252.
- 72 J. A. Champion and S. Mitragotri, Role of target geometry in phagocytosis, Proc. Natl. Acad. Sci. U. S. A., 2006, 103, 4930-4934.
- 73 G. Sharma, D. T. Valenta, Y. Altman, S. Harvey, H. Xie, S. Mitragotri and J. W. Smith, Polymer particle shape independently influences binding and internalization by macrophages, J. Controlled Release, 2010, 147, 408-412.
- 74 P. Decuzzi and M. Ferrari, The adhesive strength of nonspherical particles mediated by specific interactions, Biomaterials, 2006, 27, 5307-5314.
- 75 X. Xie, Y. Zhang, F. Li, T. Lv, Z. Li, H. Chen, L. Jia and Y. Gao, Challenges and Opportunities from Basic Cancer Biology for Nanomedicine for Targeted Drug Delivery, Curr. Cancer Drug Targets, 2019, 19, 257-276.
- 76 Y. Gao, J. Xie, H. Chen, S. Gu, R. Zhao, J. Shao and L. Jia, Nanotechnology-based intelligent drug design for cancer metastasis treatment, Biotechnol. Adv., 2014, 32, 761-777.
- 77 S. Jeyamogan, N. A. Khan and R. Siddiqui, Application and Importance of Theranostics in the Diagnosis and Treatment of Cancer, Arch. Med. Res., 2021, 52, 131-142.
- 78 M. Lamberti, S. Zappavigna, N. Sannolo, S. Porto and M. Caraglia, Advantages and risks of nanotechnologies in cancer patients and occupationally exposed workers, Expert Opin. Drug Delivery, 2014, 11, 1087-1101.
- 79 N. S. Awad, V. Paul, N. M. AlSawaftah, G. ter Haar, T. M. Allen, W. G. Pitt and G. A. Husseini, Ultrasound-Responsive

- Nanocarriers in Cancer Treatment: A Review, ACS Pharmacol. Transl. Sci., 2021, 4, 589-612.
- 80 W. He, A. C. Evans, A. Rasley, F. Bourguet, S. Peters, K. I. Kamrud, N. Wang, B. Hubby, M. Felderman, H. Gouvis, M. A. Coleman and N. O. Fischer, Cationic HDL mimetics enhance in vivo delivery of self-replicating mRNA, Nanomedicine, 2020, 24, 102154.
- 81 T. K. Ritchie, Y. V. Grinkova, T. H. Bayburt, I. G. Denisov, J. K. Zolnerciks, W. M. Atkins and S. G. Sligar, Chapter 11 -Reconstitution of membrane proteins in phospholipid bilayer nanodiscs, Methods Enzymol., 2009, 464, 211-231.
- 82 D. A. Bricarello, J. T. Smilowitz, A. M. Zivkovic, J. B. German and A. N. Parikh, Reconstituted lipoprotein: a versatile class of biologically-inspired nanostructures, ACS Nano, 2011, 5, 42-57.
- 83 N. P. Truong, M. R. Whittaker, C. W. Mak and T. P. Davis, The importance of nanoparticle shape in cancer drug delivery, Expert Opin. Drug Delivery, 2015, 12, 129-142.
- 84 L. Lin, X. Wang, X. Li, Y. Yang, X. Yue, Q. Zhang and Z. Dai, Modulating Drug Release Rate from Partially Silica-Coated Bicellar Nanodisc by Incorporating PEGylated Phospholipid, Bioconjugate Chem., 2017, 28, 53-63.
- Ravula, S. K. Ramadugu, G. Di Mauro and A. Ramamoorthy, Bioinspired, Size-Tunable Self-Assembly of Polymer-Lipid Bilayer Nanodiscs, Angew. Chem., Int. Ed., 2017, 56, 11466-11470.
- 86 T. Ravula, N. Z. Hardin, S. K. Ramadugu, S. J. Cox and A. Ramamoorthy, Formation of pH-Resistant Monodispersed Polymer-Lipid Nanodiscs, Angew. Chem., Int. Ed., 2018, 57, 1342-1345.
- 87 L. Shi, K. Howan, Q. T. Shen, Y. J. Wang, J. E. Rothman and F. Pincet, Preparation and characterization of SNAREcontaining nanodiscs and direct study of cargo release through fusion pores, Nat. Protoc., 2013, 8, 935-948.
- 88 F. Hagn, M. L. Nasr and G. Wagner, Assembly of phospholipid nanodiscs of controlled size for structural studies of membrane proteins by NMR, Nat. Protoc., 2018, 13, 79-98.
- 89 S. C. Lee, T. J. Knowles, V. L. Postis, M. Jamshad, R. A. Parslow, Y. P. Lin, A. Goldman, P. Sridhar, M. Overduin, S. P. Muench and T. R. Dafforn, A method for detergent-free isolation of membrane proteins in their local lipid environment, Nat. Protoc., 2016, 11, 1149-1162.
- 90 K. Yasuhara, S. Miki, H. Nakazono, A. Ohta and J. Kikuchi, Synthesis of organic-inorganic hybrid bicelles-lipid bilayer nanodiscs encompassed by siloxane surfaces, Chem. Commun., 2011, 47, 4691-4693.
- 91 W. Xu, P. Ling and T. Zhang, Polymeric micelles, a promising drug delivery system to enhance bioavailability of poorly water-soluble drugs, J. Drug Delivery, 2013, 2013, 340315.
- 92 M. Jones and J. Leroux, Polymeric micelles a new generation of colloidal drug carriers, Eur. J. Pharm. Biopharm., 1999, 48, 101-111.
- 93 Z. Liu, W. Jiang, J. Nam, J. J. Moon and B. Y. S. Kim, Immunomodulating Nanomedicine for Cancer Therapy, Nano Lett., 2018, 18, 6655-6659.

- 94 A. Janjic, M. Cayoren, I. Akduman, T. Yilmaz, E. Onemli, O. Bugdayci and M. E. Aribal, SAFE: A Novel Microwave Imaging System Design for Breast Cancer Screening and Early Detection-Clinical Evaluation, Diagnostics, 2021, 11, 533.
- 95 N. Jugniot, R. Bam, E. J. Meuillet, E. C. Unger and R. Paulmurugan, Current status of targeted microbubbles in diagnostic molecular imaging of pancreatic cancer, Bioeng. Transl. Med., 2021, 6, e10183.
- 96 W. S. Tummers, J. K. Willmann, B. A. Bonsing, A. L. Vahrmeijer, S. S. Gambhir and R. J. Swijnenburg, Advances in Diagnostic and Intraoperative Molecular Imaging of Pancreatic Cancer, Pancreas, 2018, 47, 675-689.
- 97 G. Zheng, J. Chen, H. Li and J. D. Glickson, Rerouting lipoprotein nanoparticles to selected alternate receptors for the targeted delivery of cancer diagnostic and therapeutic agents, Proc. Natl. Acad. Sci. U. S. A., 2005, 102, 17757-17762.
- 98 J. Rautio, H. Kumpulainen, T. Heimbach, R. Oliyai, D. Oh, T. Järvinen and J. Savolainen, Prodrugs: design and clinical applications, Nat. Rev. Drug Discovery, 2008, 7, 255-270.
- 99 X. Zhang, X. Li and Q. You, Prodrug strategy for cancer cellspecific targeting: A recent overview, Eur. J. Med. Chem., 2017, 139, 542-563.
- 100 J. Delahousse, C. Skarbek and A. Paci, Prodrugs as drug delivery system in oncology, Cancer Chemother. Pharmacol., 2019, 84, 937-958.
- 101 C. Luo, J. Sun, B. Sun and Z. He, Prodrug-based nanoparticulate drug delivery strategies for cancer therapy, Trends Pharmacol. Sci., 2014, 35, 556-566.
- 102 M. Baroud, E. Lepeltier, S. Thepot, Y. El-Makhour and O. Duval, The evolution of nucleosidic analogues: selfassembly of prodrugs into nanoparticles for cancer drug delivery, Nanoscale Adv., 2021, 3, 2157-2179.
- 103 Q. Wang, J. Guan, J. Wan and Z. Li, Disulfide based prodrugs for cancer therapy, RSC Adv., 2020, 10, 24397-24409.
- 104 X. Pang, Y. Jiang, Q. Xiao, A. W. Leung, H. Hua and C. Xu, pH-responsive polymer-drug conjugates: Design and progress, J. Controlled Release, 2016, 222, 116-129.
- 105 Y. Zeng, J. Ma, Y. Zhan, X. Xu, Q. Zeng, J. Liang and X. Chen, Hypoxia-activated prodrugs and redox-responsive nanocarriers, Int. J. Nanomed., 2018, 13, 6551-6574.
- 106 Z. Al-Ahmady and K. Kostarelos, Chemical Components for the Design of Temperature-Responsive Vesicles as Cancer Therapeutics, Chem. Rev., 2016, 116, 3883-3918.
- 107 H. Xia, Y. Zhao and R. Tong, Ultrasound-Mediated Polymeric Micelle Drug Delivery, Adv. Exp. Med. Biol., 2016, 880, 365-384.
- 108 W. Zhao, Y. Zhao, Q. Wang, T. Liu, J. Sun and R. Zhang, Remote Light-Responsive Nanocarriers for Controlled Drug Delivery: Advances and Perspectives, Small, 2019, 15, e1903060.
- 109 H. Zhang, X. L. Liu, Y. F. Zhang, F. Gao, G. L. Li, Y. He, M. L. Peng and H. M. Fan, Magnetic nanoparticles based cancer therapy: current status and applications, Sci. China: Life Sci., 2018, 61, 400-414.

- 110 H. Feng, M. Wang, C. Wu, J. Yu, D. Wang, J. Ma and J. Han, High scavenger receptor class B type I expression is related to tumor aggressiveness and poor prognosis in lung adenocarcinoma: A STROBE compliant article, Medicine, 2018, 97, e0203.
- 111 Z. Zhang, W. Cao, H. Jin, J. F. Lovell, M. Yang, L. Ding, J. Chen, I. Corbin, Q. Luo and G. Zheng, Biomimetic nanocarrier for direct cytosolic drug delivery, Angew. Chem., Int. Ed., 2009, 48, 9171-9175.
- 112 W. Cao, K. K. Ng, I. Corbin, Z. Zhang, L. Ding, J. Chen and G. Zheng, Synthesis and evaluation of a stable bacteriochlorophyll-analog and its incorporation into high-density lipoprotein nanoparticles for tumor imaging, Bioconjugate Chem., 2009, 20, 2023-2031.
- 113 K. K. Ng, J. F. Lovell, A. Vedadi, T. Hajian and G. Zheng, Self-assembled porphyrin nanodiscs with structuredependent activation for phototherapy and photodiagnostic applications, ACS Nano, 2013, 7, 3484-3490.
- 114 J. Tang, R. Kuai, W. Yuan, L. Drake, J. J. Moon and A. Schwendeman, Effect of size and pegylation of liposomes and peptide-based synthetic lipoproteins on tumor targeting, Nanomedicine, 2017, 13, 1869-1878.
- 115 W. Chen, P. A. Jarzyna, G. A. van Tilborg, V. A. Nguyen, D. P. Cormode, A. Klink, A. W. Griffioen, G. J. Randolph, E. A. Fisher, W. J. Mulder and Z. A. Fayad, RGD peptide functionalized and reconstituted high-density lipoprotein nanoparticles as a versatile and multimodal tumor targeting molecular imaging probe, FASEB J., 2010, 24, 1689-1699.
- 116 P. Wong, L. Li, J. Chea, W. Hu, E. Poku, T. Ebner, N. Bowles, J. Y. C. Wong, P. J. Yazaki, S. Sligar and J. E. Shively, Antibody Targeted PET Imaging of, Bioconjugate Chem., 2020, 31, 743-753.
- 117 D. Li, C. Hu, J. Yang, Y. Liao, Y. Chen, S. Z. Fu and J. B. Wu, Enhanced Anti-Cancer Effect of Folate-Conjugated Olaparib Nanoparticles Combined with Radiotherapy in Cervical Carcinoma, Int. J. Nanomed., 2020, 15, 10045-10058.
- 118 S. Raniolo, G. Vindigni, A. Ottaviani, V. Unida, F. Iacovelli, A. Manetto, M. Figini, L. Stella, A. Desideri and S. Biocca, Selective targeting and degradation of doxorubicin-loaded folate-functionalized DNA nanocages, Nanomedicine, 2018, 14, 1181-1190.
- 119 I. R. Corbin, J. Chen, W. Cao, H. Li, S. Lund-Katz and G. Zheng, Enhanced Cancer-Targeted Delivery Using Engineered High-Density Lipoprotein-Based Nanocarriers, J. Biomed. Nanotechnol., 2007, 3, 367-376.
- 120 I. R. Corbin, K. K. Ng, L. Ding, A. Jurisicova and G. Zheng, Near-infrared fluorescent imaging of metastatic ovarian cancer using folate receptor-targeted high-density lipoprotein nanocarriers, Nanomedicine, 2013, 8, 875-890.
- 121 A. Tahmasbi Rad, C. W. Chen, W. Aresh, Y. Xia, P. S. Lai and M. P. Nieh, Combinational Effects of Active Targeting, Shape, and Enhanced Permeability and Retention for Cancer Theranostic Nanocarriers, ACS Appl. Mater. Interfaces, 2019, 11, 10505-10519.
- 122 G. Giaccone, HER1/EGFR-targeted agents: predicting the future for patients with unpredictable outcomes to therapy, Ann. Oncol., 2005, 16, 538-548.

123 Z. Zhang, J. Chen, L. Ding, H. Jin, J. F. Lovell, I. R. Corbin, W. Cao, P. C. Lo, M. Yang, M. S. Tsao, Q. Luo and G. Zheng, HDL-mimicking peptide-lipid nanoparticles with improved tumor targeting, *Small*, 2010, **6**, 430–437.

Chem Soc Rev

- 124 P. Huda, T. Binderup, M. C. Pedersen, S. R. Midtgaard, D. R. Elema, A. Kjær, M. Jensen and L. Arleth, PET/CT Based In Vivo Evaluation of 64Cu Labelled Nanodiscs in Tumor Bearing Mice, *PLoS One*, 2015, 10, e0129310.
- 125 R. Kuai, C. Subramanian, P. T. White, B. N. Timmermann, J. J. Moon, M. S. Cohen and A. Schwendeman, Synthetic high-density lipoprotein nanodisks for targeted with alongolide delivery to adrenocortical carcinoma, *Int. J. Nanomed.*, 2017, 12, 6581–6594.
- 126 R. Kuai, L. J. Ochyl, K. S. Bahjat, A. Schwendeman and J. J. Moon, Designer vaccine nanodiscs for personalized cancer immunotherapy, *Nat. Mater.*, 2017, **16**, 489–496.
- 127 Q. Chen, G. Guan, F. Deng, D. Yang, P. Wu, S. Kang, R. Sun, X. Wang, D. Zhou, W. Dai, H. Zhang, B. He, D. Chen and Q. Zhang, Anisotropic active ligandations in siRNA-Loaded hybrid nanodiscs lead to distinct carcinostatic outcomes by regulating nano-bio interactions, *Biomaterials*, 2020, 251, 120008.
- 128 C. Pérez-Medina, J. Tang, D. Abdel-Atti, B. Hogstad, M. Merad, E. A. Fisher, Z. A. Fayad, J. S. Lewis, W. J. Mulder and T. Reiner, PET Imaging of Tumor-Associated Macrophages with 89Zr-Labeled High-Density Lipoprotein Nanoparticles, J. Nucl. Med., 2015, 56, 1272–1277.
- 129 D. Kim, S. Park, J. H. Lee, Y. Y. Jeong and S. Jon, Anti-biofouling polymer-coated gold nanoparticles as a contrast agent for in vivo X-ray computed tomography imaging, *J. Am. Chem. Soc.*, 2007, **129**, 7661–7665.
- 130 I. J. de Vries, W. J. Lesterhuis, J. O. Barentsz, P. Verdijk, J. H. van Krieken, O. C. Boerman, W. J. Oyen, J. J. Bonenkamp, J. B. Boezeman, G. J. Adema, J. W. Bulte, T. W. Scheenen, C. J. Punt, A. Heerschap and C. G. Figdor, Magnetic resonance tracking of dendritic cells in melanoma patients for monitoring of cellular therapy, *Nat. Biotechnol.*, 2005, 23, 1407–1413.
- 131 I. L. Medintz, H. T. Uyeda, E. R. Goldman and H. Mattoussi, Quantum dot bioconjugates for imaging, labelling and sensing, *Nat. Mater.*, 2005, **4**, 435–446.
- 132 D. P. Cormode, T. Skajaa, M. M. van Schooneveld, R. Koole, P. Jarzyna, M. E. Lobatto, C. Calcagno, A. Barazza, R. E. Gordon, P. Zanzonico, E. A. Fisher, Z. A. Fayad and W. J. Mulder, Nanocrystal core high-density lipoproteins: a multimodality contrast agent platform, *Nano Lett.*, 2008, 8, 3715–3723.
- 133 D. P. Cormode, E. Roessl, A. Thran, T. Skajaa, R. E. Gordon, J. P. Schlomka, V. Fuster, E. A. Fisher, W. J. Mulder, R. Proksa and Z. A. Fayad, Atherosclerotic plaque composition: analysis with multicolor CT and targeted gold nanoparticles, *Radiology*, 2010, 256, 774–782.
- 134 Y. Kim, F. Fay, D. P. Cormode, B. L. Sanchez-Gaytan, J. Tang, E. J. Hennessy, M. Ma, K. Moore, O. C. Farokhzad, E. A. Fisher, W. J. Mulder, R. Langer and Z. A. Fayad, Single step reconstitution of multifunctional

- high-density lipoprotein-derived nanomaterials using microfluidics, *ACS Nano*, 2013, 7, 9975–9983.
- 135 D. Peer, J. M. Karp, S. Hong, O. C. Farokhzad, R. Margalit and R. Langer, Nanocarriers as an emerging platform for cancer therapy, *Nat. Nanotechnol.*, 2007, 2, 751–760.
- 136 D. M. Ward, A. B. Shodeinde and N. A. Peppas, Innovations in Biomaterial Design toward Successful RNA Interference Therapy for Cancer Treatment, *Adv. Healthcare Mater.*, 2021, 10, e2100350.
- 137 M. Sadeghian, S. Rahmani, S. Khalesi and E. Hejazi, A review of fasting effects on the response of cancer to chemotherapy, *Clin. Nutr.*, 2021, **40**, 1669–1681.
- 138 B. A. Chabner and T. G. Roberts, Timeline: Chemotherapy and the war on cancer, *Nat. Rev. Cancer*, 2005, 5, 65–72.
- 139 S. Y. Qin, Y. J. Cheng, Q. Lei, A. Q. Zhang and X. Z. Zhang, Combinational strategy for high-performance cancer chemotherapy, *Biomaterials*, 2018, 171, 178–197.
- 140 M. Zhang, E. Liu, Y. Cui and Y. Huang, Nanotechnology-based combination therapy for overcoming multidrug-resistant cancer, *Cancer Biol. Med.*, 2017, **14**, 212–227.
- 141 W. J. McConathy, M. P. Nair, S. Paranjape, L. Mooberry and A. G. Lacko, Evaluation of synthetic/reconstituted highdensity lipoproteins as delivery vehicles for paclitaxel, *Anticancer Drugs*, 2008, 19, 183–188.
- 142 L. K. Mooberry, M. Nair, S. Paranjape, W. J. McConathy and A. G. Lacko, Receptor mediated uptake of paclitaxel from a synthetic high density lipoprotein nanocarrier, *J. Drug Targeting*, 2010, **18**, 53–58.
- 143 J. Jia, Y. Xiao, J. Liu, W. Zhang, H. He, L. Chen and M. Zhang, Preparation, characterizations, and in vitro metabolic processes of paclitaxel-loaded discoidal recombinant highdensity lipoproteins, *J. Pharm. Sci.*, 2012, 101, 2900–2908.
- 144 E. L. Snyder, C. C. Saenz, C. Denicourt, B. R. Meade, X. S. Cui, I. M. Kaplan and S. F. Dowdy, Enhanced targeting and killing of tumor cells expressing the CXC chemokine receptor 4 by transducible anticancer peptides, *Cancer Res.*, 2005, 65, 10646–10650.
- 145 T. Murakami, W. Wijagkanalan, M. Hashida and K. Tsuchida, Intracellular drug delivery by genetically engineered high-density lipoprotein nanoparticles, *Nano-medicine*, 2010, 5, 867–879.
- 146 W. Zhang, J. Sun, Y. Liu, M. Tao, X. Ai, X. Su, C. Cai, Y. Tang, Z. Feng, X. Yan, G. Chen and Z. He, PEG-stabilized bilayer nanodisks as carriers for doxorubicin delivery, *Mol. Pharm.*, 2014, 11, 3279–3290.
- 147 X. Zhang and B. Chen, Recombinant high density lipoprotein reconstituted with apolipoprotein AI cysteine mutants as delivery vehicles for 10-hydroxycamptothecin, *Cancer Lett.*, 2010, **298**, 26–33.
- 148 Y. Yuan, J. Wen, J. Tang, Q. Kan, R. Ackermann, K. Olsen and A. Schwendeman, Synthetic high-density lipoproteins for delivery of 10-hydroxycamptothecin, *Int. J. Nanomed.*, 2016, **11**, 6229–6238.
- 149 M. Ghosh, A. T. Singh, W. Xu, T. Sulchek, L. I. Gordon and R. O. Ryan, Curcumin nanodisks: formulation and characterization, *Nanomedicine*, 2011, 7, 162–167.

**Review Article** Chem Soc Rev

- 150 A. T. Singh, M. Ghosh, T. M. Forte, R. O. Ryan and L. I. Gordon, Curcumin nanodisk-induced apoptosis in mantle cell lymphoma, Leuk. Lymphoma, 2011, 52, 1537-1543.
- 151 C. Subramanian, P. T. White, R. Kuai, A. Kalidindi, V. P. Castle, J. J. Moon, B. N. Timmermann, A. Schwendeman and M. S. Cohen, Synthetic high-density lipoprotein nanoconjugate targets neuroblastoma stem cells, blocking migration and self-renewal, Surgery, 2018, 164, 165-172.
- 152 T. Wang, C. Subramanian, M. Yu, P. T. White, R. Kuai, J. Sanchez, J. J. Moon, B. N. Timmermann, A. Schwendeman and M. S. Cohen, Mimetic sHDL nanoparticles: A novel drugdelivery strategy to target triple-negative breast cancer, Surgery, 2019, 166, 1168-1175.
- 153 G. Gajski and V. Garaj-Vrhovac, Melittin: a lytic peptide with anticancer properties, Environ. Toxicol. Pharmacol., 2013, 36, 697-705.
- 154 J. Gao, C. Xie, M. Zhang, X. Wei, Z. Yan, Y. Ren, M. Ying and W. Lu, RGD-modified lipid disks as drug carriers for tumor targeted drug delivery, Nanoscale, 2016, 8, 7209-7216.
- 155 A. Kader and A. Pater, Loading anticancer drugs into HDL as well as LDL has little affect on properties of complexes and enhances cytotoxicity to human carcinoma cells, J. Controlled Release, 2002, 80, 29-44.
- 156 C. Subramanian, R. Kuai, Q. Zhu, P. White, J. J. Moon, A. Schwendeman and M. S. Cohen, Synthetic high-density lipoprotein nanoparticles: A novel therapeutic strategy for adrenocortical carcinomas, Surgery, 2016, 159, 284-294.
- 157 D. E. Dolmans, D. Fukumura and R. K. Jain, Photodynamic therapy for cancer, Nat. Rev. Cancer, 2003, 3, 380-387.
- 158 J. Li, H. Duan and K. Pu, Nanotransducers for Near-Infrared Photoregulation in Biomedicine, Adv. Mater., 2019, 31, e1901607.
- 159 X. L. Weng and J. Y. Liu, Strategies for maximizing photothermal conversion efficiency based on organic dyes, Drug Discovery Today, 2021, 26, 2045-2052.
- 160 Y. Ge, X. Shen, H. Cao, L. Jin, J. Shang, Y. Wang, T. Pan, Y. Yang and Z. Qi, Biological Macrocycle: Supramolecular Hydrophobic Guest Transport System Based on Nanodiscs with Photodynamic Activity, Langmuir, 2019, 35, 7824-7829.
- 161 X. Liu, X. Bao, M. Hu, H. Chang, M. Jiao, J. Cheng, L. Xie, Q. Huang, F. Li and C. Y. Li, Inhibition of PCSK9 potentiates immune checkpoint therapy for cancer, Nature, 2020, 588, 693-698.
- 162 D. M. Pardoll, The blockade of immune checkpoints in cancer immunotherapy, Nat. Rev. Cancer, 2012, 12, 252-264.
- 163 J. Duraiswamy, K. M. Kaluza, G. J. Freeman and G. Coukos, Dual blockade of PD-1 and CTLA-4 combined with tumor vaccine effectively restores T-cell rejection function in tumors, Cancer Res., 2013, 73, 3591-3603.
- 164 C. Twyman-Saint Victor, A. J. Rech, A. Maity, R. Rengan, K. E. Pauken, E. Stelekati, J. L. Benci, B. Xu, H. Dada, P. M. Odorizzi, R. S. Herati, K. D. Mansfield, D. Patsch, R. K. Amaravadi, L. M. Schuchter, H. Ishwaran, R. Mick, D. A. Pryma, X. Xu, M. D. Feldman, T. C. Gangadhar, S. M. Hahn, E. J. Wherry, R. H. Vonderheide and

- A. J. Minn, Radiation and dual checkpoint blockade activate non-redundant immune mechanisms in cancer, Nature, 2015, 520, 373-377.
- 165 C. Pfirschke, C. Engblom, S. Rickelt, V. Cortez-Retamozo, C. Garris, F. Pucci, T. Yamazaki, V. Poirier-Colame, A. Newton, Y. Redouane, Y. J. Lin, G. Wojtkiewicz, Y. Iwamoto, M. Mino-Kenudson, T. G. Huynh, R. O. Hynes, G. J. Freeman, G. Kroemer, L. Zitvogel, R. Weissleder and M. J. Pittet, Immunogenic Chemotherapy Sensitizes Tumors to Checkpoint Blockade Therapy, Immunity, 2016, 44, 343-354.
- 166 Y. Ma, S. R. Mattarollo, S. Adjemian, H. Yang, L. Aymeric, D. Hannani, J. P. Portela Catani, H. Duret, M. W. Teng, O. Kepp, Y. Wang, A. Sistigu, J. L. Schultze, G. Stoll, L. Galluzzi, L. Zitvogel, M. J. Smyth and G. Kroemer, CCL2/CCR2-dependent recruitment of functional antigenpresenting cells into tumors upon chemotherapy, Cancer Res., 2014, 74, 436-445.
- 167 G. Kroemer, L. Galluzzi, O. Kepp and L. Zitvogel, Immunogenic cell death in cancer therapy, Annu. Rev. Immunol., 2013, 31, 51-72.
- 168 R. Kuai, W. Yuan, S. Son, J. Nam, Y. Xu, Y. Fan, A. Schwendeman and J. J. Moon, Elimination of established tumors with nanodisc-based combination chemoimmunotherapy, Sci. Adv., 2018, 4, eaao1736.
- 169 P. Kadiyala, D. Li, F. M. Nuñez, D. Altshuler, R. Doherty, R. Kuai, M. Yu, N. Kamran, M. Edwards, J. J. Moon, P. R. Lowenstein, M. G. Castro and A. Schwendeman, High-Density Lipoprotein-Mimicking Nanodiscs Chemo-immunotherapy against Glioblastoma Multiforme, ACS Nano, 2019, 13, 1365-1384.
- 170 G. Parmiani, V. Russo, C. Maccalli, D. Parolini, N. Rizzo and M. Maio, Peptide-based vaccines for cancer therapy, Hum. Vaccines Immunother., 2014, 10, 3175-3178.
- 171 C. J. Melief and S. H. van der Burg, Immunotherapy of established (pre)malignant disease by synthetic long peptide vaccines, Nat. Rev. Cancer, 2008, 8, 351-360.
- 172 R. Kuai, X. Sun, W. Yuan, L. J. Ochyl, Y. Xu, A. Hassani Najafabadi, L. Scheetz, M. Z. Yu, I. Balwani, A. Schwendeman and J. J. Moon, Dual TLR agonist nanodiscs as a strong adjuvant system for vaccines and immunotherapy, J. Controlled Release, 2018, 282, 131-139.
- 173 R. Kuai, X. Sun, W. Yuan, Y. Xu, A. Schwendeman and J. J. Moon, Subcutaneous Nanodisc Vaccination with Neoantigens for Combination Cancer Immunotherapy, Bioconjugate Chem., 2018, 29, 771-775.
- 174 E. Batlle and H. Clevers, Cancer stem cells revisited, Nat. Med., 2017, 23, 1124-1134.
- 175 S. Liu, Y. Cong, D. Wang, Y. Sun, L. Deng, Y. Liu, R. Martin-Trevino, L. Shang, S. P. McDermott, M. D. Landis, S. Hong, A. Adams, R. D'Angelo, C. Ginestier, E. Charafe-Jauffret, S. G. Clouthier, D. Birnbaum, S. T. Wong, M. Zhan, J. C. Chang and M. S. Wicha, Breast cancer stem cells transition between epithelial and mesenchymal states reflective of their normal counterparts, Stem Cell Rep., 2014, 2, 78-91.
- 176 A. Hassani Najafabadi, J. Zhang, M. E. Aikins, Z. I. Najaf Abadi, F. Liao, Y. Qin, E. B. Okeke, L. M. Scheetz, J. Nam,

- Y. Xu, D. Adams, P. Lester, T. Hetrick, A. Schwendeman, M. S. Wicha, A. E. Chang, Q. Li and J. J. Moon, Cancer Immunotherapy via Targeting Cancer Stem Cells Using Vaccine Nanodiscs, Nano Lett., 2020, 20, 7783-7792.
- 177 L. Scheetz, P. Kadiyala, X. Sun, S. Son, A. Hassani Najafabadi, M. Aikins, P. R. Lowenstein, A. Schwendeman, M. G. Castro and J. J. Moon, Synthetic High-density Lipoprotein Nanodiscs for Personalized Immunotherapy Against Gliomas, Clin. Cancer Res., 2020, 26, 4369-4380.
- 178 V. Singh, N. Khan and G. R. Jayandharan, Vector engineering, strategies and targets in cancer gene therapy, Cancer Gene Ther., 2021, DOI: 10.1038/s41417-021-00331-7.
- 179 W. Sun, Q. Shi, H. Zhang, K. Yang, Y. Ke, Y. Wang and L. Qiao, Advances in the techniques and methodologies of cancer gene therapy, Discovery Med., 2019, 27, 45-55.
- 180 M. M. Shahzad, L. S. Mangala, H. D. Han, C. Lu, J. Bottsford-Miller, M. Nishimura, E. M. Mora, J. W. Lee, R. L. Stone, C. V. Pecot, D. Thanapprapasr, J. W. Roh, P. Gaur, M. P. Nair, Y. Y. Park, N. Sabnis, M. T. Deavers, J. S. Lee, L. M. Ellis, G. Lopez-Berestein, W. J. McConathy, L. Prokai, A. G. Lacko and A. K. Sood, Targeted delivery of small interfering RNA using reconstituted high-density lipoprotein nanoparticles, Neoplasia, 2011, 13, 309-319.
- 181 A. Del Pozo-Rodríguez, M. Solinís and A. Rodríguez-Gascón, Applications of lipid nanoparticles in gene therapy, Eur. J. Pharm. Biopharm., 2016, 109, 184-193.
- 182 L. Aagaard and J. J. Rossi, RNAi therapeutics: principles, prospects and challenges, Adv. Drug Delivery Rev., 2007, 59, 75-86.
- 183 F. Y. Xie, M. C. Woodle and P. Y. Lu, Harnessing in vivo siRNA delivery for drug discovery and therapeutic development, Drug Discovery Today, 2006, 11, 67-73.
- 184 P. Yue and J. Turkson, Targeting STAT3 in cancer: how successful are we?, Expert Opin. Invest. Drugs, 2009, 18, 45-56.
- 185 J. E. Darnell, STATs and gene regulation, Science, 1997, 277, 1630-1635.
- 186 M. Ghosh, G. Ren, J. B. Simonsen and R. O. Ryan, Cationic lipid nanodisks as an siRNA delivery vehicle, Biochem. Cell Biol., 2014, 92, 200-205.
- 187 K. M. McMahon, M. P. Plebanek and C. S. Thaxton, Properties of Native High-Density Lipoproteins Inspire Synthesis of Actively Targeted, Adv. Funct. Mater., 2016, 26, 7824-7835.
- 188 J. L. Huang, G. Jiang, Q. X. Song, X. Gu, M. Hu, X. L. Wang, H. H. Song, L. P. Chen, Y. Y. Lin, D. Jiang, J. Chen, J. F. Feng, Y. M. Qiu, J. Y. Jiang, X. G. Jiang, H. Z. Chen and X. L. Gao, Lipoprotein-biomimetic nanostructure enables efficient targeting delivery of siRNA to Rasactivated glioblastoma cells via macropinocytosis, Nat. Commun., 2017, 8, 15144.
- 189 C. Wolfrum, S. Shi, K. N. Jayaprakash, M. Jayaraman, G. Wang, R. K. Pandey, K. G. Rajeev, T. Nakayama, K. Charrise, E. M. Ndungo, T. Zimmermann, V. Koteliansky, M. Manoharan and M. Stoffel, Mechanisms and optimization of in vivo delivery of lipophilic siRNAs, Nat. Biotechnol., 2007, 25, 1149-1157.

- 190 Y. Ding, W. Wang, M. Feng, Y. Wang, J. Zhou, X. Ding, X. Zhou, C. Liu, R. Wang and Q. Zhang, A biomimetic nanovector-mediated targeted cholesterol-conjugated siRNA delivery for tumor gene therapy, Biomaterials, 2012, 33, 8893-8905.
- 191 L. Lin, X. Wang, Y. Guo, K. Ren, X. Li, L. Jing, X. Yue, Q. Zhang and Z. Dai, Hybrid bicelles as a pH-sensitive nanocarrier for hydrophobic drug delivery, RSC Adv., 2016, 6, 79811-79821.
- 192 Y. Kazuma, H. Hiroki and K. Jun-ichi, Thermal Stability of Synthetic Lipid Bicelles Encompassed by Siloxane Surfaces as Organic-Inorganic Hybrid Nanodiscs, Chem. Lett., 2012, 41, 1223-1225.
- 193 M. Ikeda, T. Nakamura, Y. Nagase, K. Ikeda and Y. Sekine, Thermal degradation of poly[(tetramethyl-p-silphenylene) siloxane], J. Polym. Sci., Polym Chem. Ed., 1981, 19, 2595-2607.
- 194 G. Ducom, B. Laubie, A. Ohannessian, C. Chottier, P. Germain and V. Chatain, Hydrolysis of polydimethylsiloxane fluids in controlled aqueous solutions, Water Sci. Technol., 2013, 68, 813-820.
- 195 I. Blanco, Polysiloxanes in Theranostics and Drug Delivery: A Review, Polymers, 2018, 10, 755.
- 196 M. Marguet, C. Bonduelle and S. Lecommandoux, Multicompartmentalized polymeric systems: towards biomimetic cellular structure and function, Chem. Soc. Rev., 2013, 42, 512-529.
- 197 D. E. Discher and A. Eisenberg, Polymer vesicles, Science, 2002, 297, 967-973.
- 198 S. Igbal, M. Blenner, A. Alexander-Bryant and J. Larsen, Polymersomes for Therapeutic Delivery of Protein and Nucleic Acid Macromolecules: From Design to Therapeutic Applications, Biomacromolecules, 2020, 21, 1327-1350.
- 199 X. Hu, Y. Zhang, Z. Xie, X. Jing, A. Bellotti and Z. Gu, Stimuli-Responsive Polymersomes for Biomedical Applications, Biomacromolecules, 2017, 18, 649-673.
- 200 Y. Yu, L. Zhang and A. Eisenberg, Multiple Morphologies of Crew-Cut Aggregates of Polybutadiene-b-poly(acrylic acid) Diblocks with Low Tg Cores, Langmuir, 1997, 13, 2578-2581.
- 201 M. Antonietti and S. Forster, Vesicles and liposomes: A self-assembly principle beyond lipids, Adv. Mater., 2003, 15, 1323-1333.
- 202 A. Blanazs, S. P. Armes and A. J. Ryan, Self-Assembled Block Copolymer Aggregates: From Micelles to Vesicles and their Biological Applications, Macromol. Rapid Commun., 2009, 30, 267-277.
- 203 E. D. Dennis and A. Fariyal, Polymersomes, Ann. Rev. Biomed. Eng., 2006, 8, 323-341.
- 204 J. C. Lee, H. Bermudez, B. M. Discher, M. A. Sheehan, Y. Y. Won, F. S. Bates and D. E. Discher, Preparation, stability, and in vitro performance of vesicles made with diblock copolymers, Biotechnol. Bioeng., 2001, 73, 135-145.
- 205 H. Kim, Y. J. Kang, S. Kang and K. T. Kim, Monosaccharide-responsive release of insulin from polymersomes of polyboroxole block copolymers at neutral pH, J. Am. Chem. Soc., 2012, 134, 4030-4033.

206 Z. Fu, M. A. Ochsner, H. P. de Hoog, N. Tomczak and M. Nallani, Multicompartmentalized polymersomes for selective encapsulation of biomacromolecules, Chem. Commun., 2011, 47, 2862-2864.

**Review Article** 

- 207 F. Ahmed and D. E. Discher, Self-porating polymersomes of PEG-PLA and PEG-PCL: hydrolysis-triggered controlled release vesicles, J. Controlled Release, 2004, 96, 37-53.
- 208 Y. Zhang, F. Wu, W. Yuan and T. Jin, Polymersomes of asymmetric bilayer membrane formed by phase-guided assembly, J. Controlled Release, 2010, 147, 413-419.
- 209 Q. Liu, H. Zhu, J. Qin, H. Dong and J. Du, Theranostic vesicles based on bovine serum albumin and poly(ethylene glycol)-block-poly(L-lactic-co-glycolic acid) for magnetic resonance imaging and anticancer drug delivery, Biomacromolecules, 2014, 15, 1586-1592.
- 210 W. Hou, R. Liu, S. Bi, Q. He, H. Wang and J. Gu, Photo-Responsive Polymersomes as Drug Delivery System for Potential Medical Applications, Molecules, 2020, 25, 542-552.
- 211 L. Pourtau, H. Oliveira, J. Thevenot, Y. Wan, A. R. Brisson, O. Sandre, S. Miraux, E. Thiaudiere and S. Lecommandoux, Antibody-functionalized magnetic polymersomes: in vivo targeting and imaging of bone metastases using high resolution MRI, Adv. Healthcare Mater., 2013, 2, 1420-1424.
- 212 Y. Zou, F. Meng, C. Deng and Z. Zhong, Robust, tumorhoming and redox-sensitive polymersomal doxorubicin: A superior alternative to Doxil and Caelyx?, J. Controlled Release, 2016, 239, 149-158.
- 213 E. A. Scott, A. Stano, M. Gillard, A. C. Maio-Liu, M. A. Swartz and J. A. Hubbell, Dendritic cell activation and T cell priming with adjuvant- and antigen-loaded oxidation-sensitive polymersomes, Biomaterials, 2012, 33, 6211-6219.
- 214 J. Du, Y. Tang, A. L. Lewis and S. P. Armes, pH-sensitive vesicles based on a biocompatible zwitterionic diblock copolymer, J. Am. Chem. Soc., 2005, 127, 17982-17983.
- 215 J. Zhang, L. Wu, F. Meng, Z. Wang, C. Deng, H. Liu and Z. Zhong, pH and reduction dual-bioresponsive polymersomes for efficient intracellular protein delivery, Langmuir, 2012, 28, 2056-2065.
- 216 C. J. Mable, R. R. Gibson, S. Prevost, B. E. McKenzie, O. O. Mykhaylyk and S. P. Armes, Loading of Silica Nanoparticles in Block Copolymer Vesicles during Polymerization-Induced Self-Assembly: Encapsulation Efficiency and Thermally Triggered Release, J. Am. Chem. Soc., 2015, 137, 16098-16108.
- 217 L. Wang, G. Liu, X. Wang, J. Hu, G. Zhang and S. Liu, Acid-Disintegratable Polymersomes of pH-Responsive Amphiphilic Diblock Copolymers for Intracellular Drug Delivery, Macromolecules, 2015, 48, 7262-7272.
- 218 A. Koide, A. Kishimura, K. Osada, W. D. Jang, Y. Yamasaki and K. Kataoka, Semipermeable polymer vesicle (PICsome) self-assembled in aqueous medium from a pair of oppositely charged block copolymers: physiologically stable micro-/nanocontainers of water-soluble macromolecules, J. Am. Chem. Soc., 2006, 128, 5988-5989.

- 219 A. Moquin, J. Ji, K. Neibert, F. M. Winnik and D. Maysinger, Encapsulation and Delivery of Neutrophic Proteins and Hydrophobic Agents Using PMOXA-PDMS-PMOXA Triblock Polymersomes, ACS Omega, 2018, 3,
- 220 X. Y. Xiong, Y. P. Li, Z. L. Li, C. L. Zhou, K. C. Tam, Z. Y. Liu and G. X. Xie, Vesicles from Pluronic/poly(lactic acid) block copolymers as new carriers for oral insulin delivery, J. Controlled Release, 2007, 120, 11-17.
- 221 A. Wittemann, T. Azzam and A. Eisenberg, Biocompatible polymer vesicles from biamphiphilic triblock copolymers and their interaction with bovine serum albumin, Langmuir, 2007, 23, 2224-2230.
- 222 G. Liu, S. Ma, S. Li, R. Cheng, F. Meng, H. Liu and Z. Zhong, The highly efficient delivery of exogenous proteins into cells mediated by biodegradable chimaeric polymersomes, Biomaterials, 2010, 31, 7575-7585.
- 223 B. Li, G. Chen, F. Meng, T. Li, J. Yue, X. Jing and Y. Huang, A novel amphiphilic copolymer poly(ethylene oxide-co-allyl glycidyl ether)-graft-poly(ε-caprolactone): synthesis, selfassembly, and protein encapsulation behavior, Polym. Chem., 2012, 3, 2421-2429.
- 224 B. Li, Y. Qi, S. He, Y. Wang, Z. Xie, X. Jing and Y. Huang, Asymmetric copolymer vesicles to serve as a hemoglobin vector for ischemia therapy, Biomater. Sci., 2014, 2, 1254-1261.
- 225 Y. Wang, L. Yan, B. Li, Y. Qi, Z. Xie, X. Jing, X. Chen and Y. Huang, Protein-Resistant Biodegradable Amphiphilic Graft Copolymer Vesicles as Protein Carriers, Macromol. Biosci., 2015, 15, 1304-1313.
- 226 H. Xu, F. Meng and Z. Zhong, Reversibly crosslinked temperature-responsive nano-sized polymersomes: synthesis and triggered drug release, J. Mater. Chem., 2009, 19, 4183-4190.
- 227 T. Anajafi and S. Mallik, Polymersome-based drug-delivery strategies for cancer therapeutics, Ther. Delivery, 2015, 6, 521-534.
- 228 F. Meng, Z. Zhong and J. Feijen, Stimuli-responsive polymersomes for programmed drug delivery, Biomacromolecules, 2009, 10, 197-209.
- 229 D. Zhou, Z. Fei, L. Jin, P. Zhou, C. Li, X. Liu and C. Zhao, Dual-responsive polymersomes as anticancer drug carriers for the co-delivery of doxorubicin and paclitaxel, J. Mater. Chem. B, 2021, 9, 801-808.
- 230 T. Thambi, J. H. Park and D. S. Lee, Stimuli-responsive polymersomes for cancer therapy, Biomater. Sci., 2016, 4, 55-69.
- 231 D. Gigmes and T. Trimaille, Advances in amphiphilic polylactide/vinyl polymer based nano-assemblies for drug delivery, Adv. Colloid Interface Sci., 2021, 294, 102483.
- 232 Y. Ramot, M. Haim-Zada, A. J. Domb and A. Nyska, Biocompatibility and safety of PLA and its copolymers, Adv. Drug Delivery Rev., 2016, 107, 153-162.
- 233 B. Pang, Y. Yu and W. Zhang, Thermoresponsive Polymers Based on Tertiary Amine Moieties, Macromol. Rapid Commun., 2021, e2100504.

234 P. Flemming, A. S. Münch, A. Fery and P. Uhlmann, Constrained thermoresponsive polymers - new insights into fundamentals and applications, Beilstein J. Org. Chem., 2021, 17, 2123-2163.

Chem Soc Rev

- 235 H. Liu, J. Yao, H. Guo, X. Cai, Y. Jiang, M. Lin, X. Jiang, W. Leung and C. Xu, Tumor Microenvironment-Responsive Nanomaterials as Targeted Delivery Carriers for Photodynamic Anticancer Therapy, Front. Chem., 2020, 8, 758.
- 236 P. Mi, Stimuli-responsive nanocarriers for drug delivery, tumor imaging, therapy and theranostics, Theranostics, 2020, 10, 4557-4588.
- 237 H. Park, G. Saravanakumar, J. Kim, J. Lim and W. J. Kim, Tumor Microenvironment Sensitive Nanocarriers for Bioimaging and Therapeutics, Adv. Healthcare Mater., 2021, 10, e2000834.
- 238 S. Wang, G. Yu, Z. Wang, O. Jacobson, R. Tian, L. S. Lin, F. Zhang, J. Wang and X. Chen, Hierarchical Tumor Microenvironment-Responsive Nanomedicine for Programmed Delivery of Chemotherapeutics, Adv. Mater., 2018, 30, e1803926.
- 239 M. Tanaka, A. Hosotani, Y. Tachibana, M. Nakano, K. Iwasaki, T. Kawakami and T. Mukai, Preparation and Characterization of Reconstituted Lipid-Synthetic Polymer Discoidal Particles, Langmuir, 2015, 31, 12719-12726.
- 240 K. Georgila, D. Vyrla and E. Drakos, Apolipoprotein A-I (ApoA-I), Immunity, Inflammation and Cancer, Cancers, 2019, 11, 1097.
- 241 A. O. Oluwole, B. Danielczak, A. Meister, J. O. Babalola, C. Vargas and S. Keller, Solubilization of Membrane Proteins into Functional Lipid-Bilayer Nanodiscs Using a

- Diisobutylene/Maleic Acid Copolymer, Angew. Chem., Int. Ed., 2017, 56, 1919-1924.
- 242 M. C. Fiori, W. Zheng, E. Kamilar, G. Simiyu, G. A. Altenberg and H. Liang, Extraction and reconstitution of membrane proteins into lipid nanodiscs encased by zwitterionic styrene-maleic amide copolymers, Sci. Rep., 2020, 10, 9940.
- 243 N. Avramovic, B. Mandic, A. Savic-Radojevic and T. Simic, Polymeric Nanocarriers of Drug Delivery Systems in Cancer Therapy, Pharmaceutics, 2020, 12, 298.
- 244 R. Duncan, Polymer conjugates as anticancer nanomedicines, Nat. Rev. Cancer, 2006, 6, 688-701.
- 245 J. H. Park, S. Lee, J. H. Kim, K. Park, K. Kim and I. C. Kwon, Polymeric nanomedicine for cancer therapy, Prog. Polym. Sci., 2008, 33, 113-137.
- 246 X. Qin and Y. S. Li, Strategies To Design and Synthesize Polymer-Based Stimuli-Responsive Drug-Delivery Nanosystems, ChemBioChem, 2020, 21, 1236-1253.
- 247 R. Wen, A. C. Umeano, P. P. Chen and A. A. Farooqi, Polymer-Based Drug Delivery Systems for Cancer, Crit. Rev. Ther. Drug, 2018, 35, 521-553.
- 248 Y. Hui, X. Yi, F. Hou, D. Wibowo, F. Zhang, D. Zhao, H. Gao and C. X. Zhao, Role of Nanoparticle Mechanical Properties in Cancer Drug Delivery, ACS Nano, 2019, 13, 7410-7424.
- 249 S. Sindhwani, A. M. Syed, J. Ngai, B. R. Kingston, L. Maiorino, J. Rothschild, P. MacMillan, Y. Zhang, N. U. Rajesh, T. Hoang, J. L. Y. Wu, S. Wilhelm, A. Zilman, S. Gadde, A. Sulaiman, B. Ouyang, Z. Lin, L. Wang, M. Egeblad and W. C. W. Chan, The entry of nanoparticles into solid tumours, Nat. Mater., 2020, 19, 566-575.